IJCRT.ORG ISSN : 2320-2882

INTERNATIONAL JOURNAL OF CREATIVE RESEARCH THOUGHTS (IJCRT)

An International Open Access, Peer-reviewed, Refereed Journal

STRENGTH-PERFORMANCE CORRELATION FACTOR FOR SIESMIC DESIGN OF INFILLED MOMENT RESISTING RC FRAMES

[1]Feras Ahmed, [2]Ayman Embaby, [3]Ayman Hussein

[1]Post Graduate Student, [2]Professor of Structural Engineer, [3]Professor of Structural Engineer

[1]Departement of Structural Engineering,

[1]Ain Shams University, Cairo, Egypt

Abstract: Unreinforced masonry (URM) infills are seldom included in numerical analysis of reinforced concrete structural systems, and are generally considered as non-structural components. On the contrary, masonry infills can increase the strength, stiffness, and energy dissipation of concrete structures; whilst drastically helping in reducing the deformations and hence ductility demands for the structural members. But owing to the complexity they introduce to analysis, they are generally kept unaccounted for. This paper however, reviews the effects of (URM) infills on 2D frames using performance-based design (PBD) approach, by developing a performance factor (P) for different performance levels. Regular 2D-infilled frames of different heights and infill percentages are assessed using this approach through a non-linear static pushover analysis. Conventional building seismic codes are based on a linear force-based design (FBD) approach to ensure satisfactory performance of structures during earthquakes. Seismic forces are reduced by a response modification factor (R), which is related to the structure's ability to undergo inelastic deformations and to dissipate the earthquake input energy through hysteretic behavior. Herein, (FBD) approach is strength based rather than a displacement based design. While however, performance criterion in the performance-based design (PBD) approach is usually displacement based providing a better view on the performance of the structure and predicting the expected non-linear response during seismic events. A new factor namely the performance factor (P) is presented in this paper, by carrying out a correlation between force-based and performance-based design methods, to be used in designing RC structures whilst fulfilling different performance levels intended by the owner.

Index Terms **– Seismic Analysis, Non-linear Pushover Analysis, Performance Factor, Response Modification Factor, Masonry Infills, RC Moment Resisting Frames**

I. INTRODUCTION

Conventional seismic analysis of structure, linear force-based design (FBD), incorporates only elastic response of the structure. To understand nonlinear response of the structure, Performance Based Design (PBD) approach is widely used. PBD includes Pushover analysis i.e. nonlinear static analysis, which shows the post-elastic behavior of the structure. Performance based design (PBD) has been deemed as one of the most promising design methods in the past few decades. PBD was initiated in 1980s in the United States [Hamburger et al., 2004]. Engineers have been practicing PBD for several decades since then, and different structural performance concept guidelines were developed through the years [ASCE 2007, 2014; ATC 1996; FEMA 1997, 2000, 2005; TBI 2017]. The current PBD mainly has two advantages over the traditional force-based design (FBD). Firstly, PBD reduces the uncertainties in the FBD and, secondly, demonstrates the performance levels (immediate occupancy level, life safety level, and collapse prevention level) of the structure, using measurable criteria. This in return helps engineers to design structures based on the performance level required by the owner, hence providing more cost-effective solutions.

1.1 Influence of URM Walls during Earthquakes

The presence of unreinforced masonry (URM) infills enhances the capacity of a building to resist lateral forces. Many existing buildings that have been designed according to older codes, that did not include specific regulations for ductile design, behave nonetheless satisfactorily during earthquakes, such that of the 1992 Cairo earthquake, for which they are supposed to fail according to modern concepts. This is due to the available margin of safety for lateral strength owing to the presence of infills that were not taken into account in the initial calculations, increasing the lateral stiffness, strength, overall ductility and energy dissipation capacity. In general it is on the safe side to omit the presence of infills in the design of a building.

Irregular distribution of masonry infills, though, may result in increased demand for lateral resistance of a building as compared to bare structure with no infills. The asymmetric layout of infills in plan is in general considered less serious than the irregularity in height, which might result to soft stories and short column effects, which in turn could be a serious concern. For instance, in the Jabalpur earthquake of 1997 in India [Jain et al., 1997], the only RC frame buildings that sustained damage were those with soft-first storey created by the absence of infills in the ground storey, facilitating a parking.

The seismic design of (URM) infilled RC frame structures is handled in different ways across the world. Some of the prevalent design practices are,

- Infills are adequately separated from the RC frame, and hence do not interfere with the frame under lateral deformations. Thus, the entire lateral force on the building is carried by the bare RC frame alone.
- Infills are built integral with the RC frame, but considered as non-structural elements. The lateral force is also carried by the bare RC frame alone. This is the most common design practice in the developing countries.
- Infills are built integral with the RC frame, and considered as structural elements. The in-plane stiffness offered by the infill walls is considered in the analysis of the building; and the forces from this analysis are used in the design of RC frame members and joints [CEN, 1994; NBC 201, 1994].

A significant number of experiments and analytical researches have been expended till date in understanding the behavior of masonry infilled frames [CEB, 1996]. Infills interfere with the lateral deformations of the RC frame, where separation of frame and infill takes place along one diagonal resulting to the formation of a compression strut along the other. Thus, infills add lateral stiffness to the building, and the structural load transfer mechanism is changed from frame action to predominant truss action. The frame columns now experience increased axial forces but with reduced bending moments and shear forces.

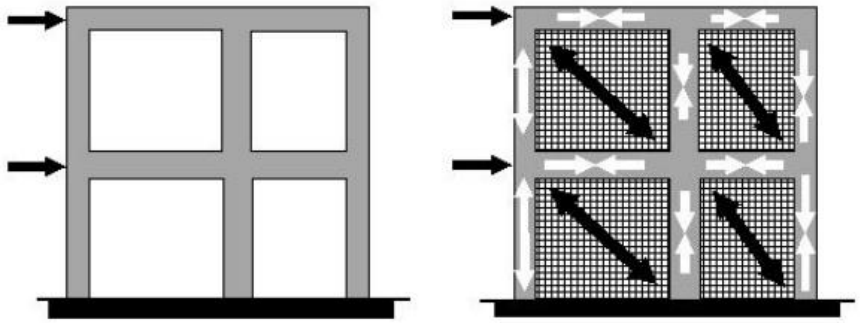

Figure 1: Change in the lateral load transfer mechanism owing to inclusion of masonry infill walls

1.2 Response Modification Factor (R)

Response modification factor (R) is used to scale down the elastic response of the structure to accommodate for its inelastic behavior under lateral loading. The structure is allowed to be damaged to certain extents in case of severe shaking. Hence, structures are designed for seismic forces much less than what are expected under strong shaking, providing more practical and economical design solutions. The concept of R factor was based on the premise that well-detailed seismic framing systems could sustain large inelastic deformations without collapse.

ECP-201 suggests R factors 5 and 7 for RC moment-resisting frames with limited ductility and RC moment-resisting frames with sufficient ductility respectively. The basic concept of R factor is that: if R=5 used to design RC frame, then it is to facilitate that such frame can take only $1/5^{th}$ of the actual seismic forces, while additional forces or deflection can be accommodated by the ductile capacity of frames. In the conventional analysis, structures are never designed for the ductile part, but only follow ductile detailing guidelines as per ECP-203. ECP-201 and ECP-203 do not provide guidelines to calculate the components of the R factor. Thus, non-linear static analysis is required to determine the R components.

The value of R factor mainly depends on the lateral load resisting system and the structural geometry of a building; different codes, though, could provide slightly different values of R for the same system as compared to one another. This is mainly to the ductile detailing guidelines followed by each code and the definition of each system. Nonetheless, all codes follow the same conventional methodology of FBD.

Table 1: R factor as per different codes

Lateral Load Resisting System	**R- Factor**			
	ECP-201	IS 1893-2002	UBC-97	IBC-2003
RC moment-resisting frames with limited ductility	5	-	-	-
RC moment-resisting frames with Sufficient ductility	7	-	-	-
Ordinary Moment resisting frames (OMRF)	-	3	4.5	3
Intermediate Moment resisting frame (SMRF)	-	-	5.5	5
Special Moment resisting frame (SMRF)	-	5	8.5	8

II. METHODOLOGY

Pushover analysis is a tool to perform non-linear static analysis (NSA) by subjecting a monotonically increasing pattern of lateral load on the structure, representing the forces to be experienced by the structure during an earthquake. Under incrementally increasing loads, various structural elements may yield sequentially, resulting to loss in the structure's stiffness. A non-linear force-displacement relationship curve, namely pushover curve, is derived evaluating the mechanism of plastic hinge formation at every stage in the post-elastic region. The analysis is terminated when the target displacement or critical state is reached. In this paper, ETABS 17 was used in the analysis procedure. ETABS defines plastic hinge properties as per FEMA-356. Hinge property is defined in the form of a force-deformation curve with five points labelled A, B, C, D, and E as shown below. The value of these points obtained from the moment-curvature relationship of an element depends on the material property, geometry, longitudinal reinforcement, shear reinforcement and loads subjected on the element.

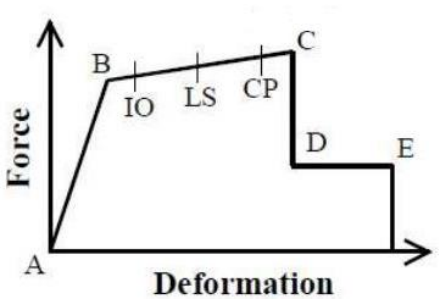

Figure 2: Force-deformation for hinge properties

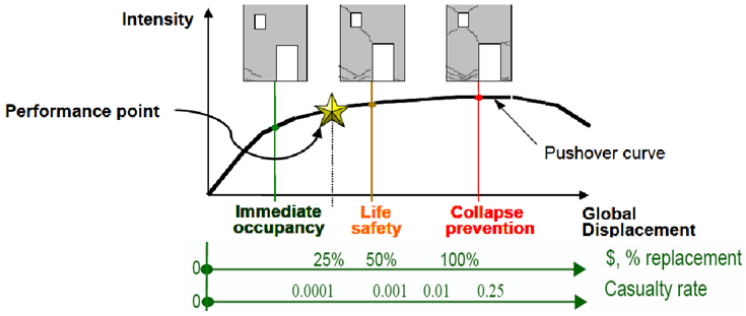

Figure 3: Performance objectives for NSA

Performance-based design (PBD) approach mainly evaluates the performance of a structure under seismic loading. The performance objectives lay between a range of predetermined limits rather than a discrete value. In most PBD guidelines, three performance levels are defined and which would be followed in this paper.

- Immediate Occupancy (IO): Performance required for high seismic hazard level with a 50% probability of occurrence in 50 years; facility continues in operation with negligible damage.
- Life Safety (LS): Performance required for moderate seismic hazard level with a 10% probability of occurrence in 50 years; damage is moderated to extensive.
- Collapse Prevention (CP): Performance required for low seismic hazard level with a 2% probability of occurrence in 50 years; damage is severe and life safety could be at risk, however structural collapse is prevented.

2.1 NSA Methodologies adopted by Different Guidelines

Different methods have been adopted by different guidelines throughout the years to predict the target displacement of a structure, including Capacity Spectrum Method (CSM) [ATC-40, EC8] and Displacement Coefficient Method (DCM) [FEMA-356]. According to the CSM method [ATC-40, EC8], a performance point is achieved by plotting a capacity spectrum curve, acceleration-displacement response spectrum curve (ADRS), developed from the pushover curve, force-displacement curve, against the reduced demand curve. The graphical intersection between the two curves is the performance point, which approximates the response of the structure during a seismic event.

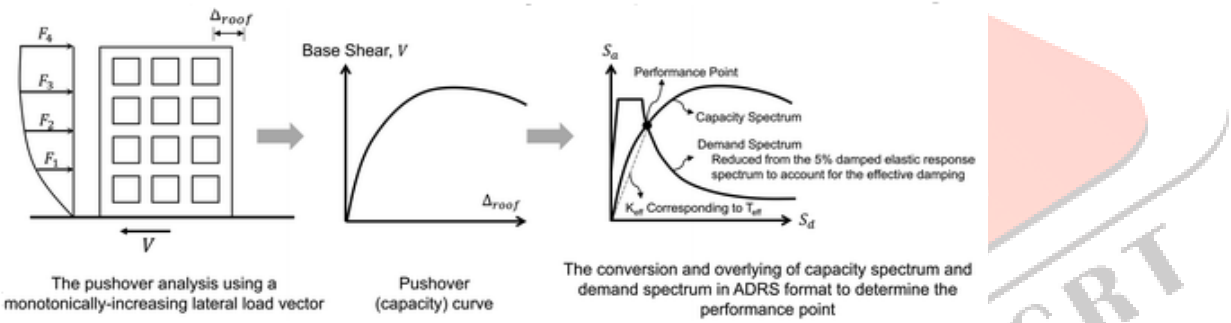

Figure 4: Overall process of the capacity spectrum method (CSM)

DCM method [FEMA-356], on the other hand, provides a simple method to estimate the target displacement, without the need to convert the pushover curve into its corresponding spectral coordinates as the CSM method. Consequently, a more comprehensive improved version of both the CSM and DCM methods has been developed as per FEMA-440 report. The report proposes a more efficient bilinear approximation for the pushover curve and an improvement in the expressions used to estimate the effective time period and effective viscous damping for reducing the elastic demand curve in the CSM method; while also improving the displacement modifying coefficients for the DCM method. This improved procedure was later implemented in ASCE/SEI 41-06 (2007) and ASCE/SEI 41-13 (2013).

2.2 Calculation of R and P Factors

In this paper, the performance factor (P) will be calculated using similar procedure used to calculate the response modification factor (R); where different height frames with variable infill percentages will be used to assess the P factor matching different performance levels. In the mid-1980s, Berkeley described R as the product of three factors that accounted for reserve strength, ductility, and added viscous damping.

$$R = R_{\Omega}.R_{\mu}.R_{\xi} \quad (1)$$

Where R_{Ω} stands for over-strength, R_{μ} for ductility, and R_{ξ} for damping factors respectively. ATC-19 then concluded by splitting the R into three similar components with replacing R_{ξ} with R_R, redundancy factor.

2.2.1 Over-strength Factor (R_{Ω})

The additional strength beyond the design strength is called the over-strength. Most structures display considerable over-strength. Sequential yielding of critical regions, members' size or reinforcement lager than required, strain hardening in materials, confinement of concrete, strength contribution of non-structural elements, load factors and multiple load cases, and the difference between the actual and design material strength are all sources of over-strength. Over-strength factor can be idealized as:

Ω = apparent max strength/design strength.

$$\Omega = V_u/V_d \quad (2)$$

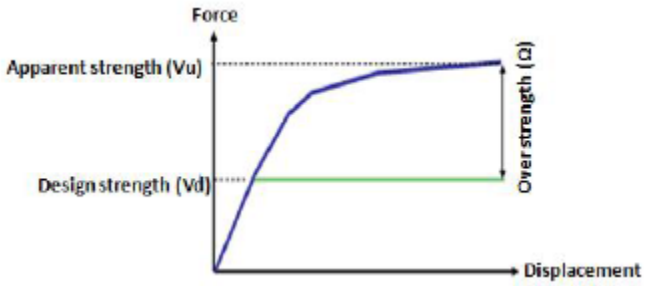

Figure 5: Force displacement relationship for over-strength

2.2.2 Ductility Reduction Factor (R_μ)

The ductility reduction factor (Rμ) is a factor which reduces the elastic force to idealized yield strength level of the structure. It can be calculated using ductility (μ) of the structure, which is the capacity of the structure, or its members, to undergo large inelastic deformations without significant loss of strength or stiffness, resulting to dissipation of large amounts of energy. Ductility (μ) is represented by the ratio of maximum roof displacement (δ_u) to its yield displacement (δ_y). According to FEMA-P695, maximum roof displacement (δ_u) can be assumed to be the value at which the structure loses 80% of its base shear capacity, $0.8V_{max}$, as shown in the figure below.

$$\mu = \delta_u/\delta_y \quad (3)$$

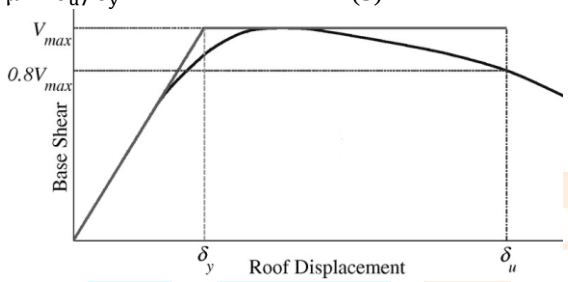

Figure 6: Idealized nonlinear static pushover curve

The relationship linking displacement ductility (μ) and ductility-dependent reduction factor (R_μ) factor has been the subject of considerable research and various methods were suggested to calculate the ductility reduction factor (R_μ), including [Newmark and Hall (1982), Krawinkler and Nassar (1992), Miranda and Bertero (1994)]. In this study, ductility factor is considered using Newmark and Hall (1982) method, where the relationship for R_μ as a function of μ, for short, intermediate and long period structures is derived as follows.

$$R_\mu = 1 \quad \text{For } T \leq 0.2 \text{ seconds} \quad (4)$$

$$R_\mu = \sqrt{2\mu - 1} \quad \text{For } 0.2 < T \leq 0.5 \text{ seconds} \quad (5)$$

$$R_\mu = \mu \quad \text{For } T > 0.5 \text{ seconds} \quad (6)$$

2.2.3 Redundancy Reduction Factor (R_R)

Redundancy is usually used to define the reliability of the structure to withstand lateral loading. Hence, structures with a high degree of redundancy would have better lateral load resistance. In a non-redundant system, the failure of a member is equivalent to the failure of the entire structure; however in a redundant system, failure will occur if more than one member fails. Thus, the reliability of a system is a function of the system's redundancy.

Table 2: Redundancy Factor (R_R) according to ATC

Lines of vertical seismic framing	Draft redundancy factor
2	0.71
3	0.86
4	1.00

2.3 Modelling of Infill Walls

The masonry infill walls are usually modelled as equivalent diagonal compression strut. In this method the infill wall is idealized as diagonal strut and the frame is modelled a truss element. FEMA-306 recommends the following equations, which represents the in-plane stiffness of solid unreinforced masonry infill panel before cracking. Where the properties of diagonal compression strut where the area (A_e) as a function of the width of the strut (W_e) and the thickness of the infill panel (t) can be written as:

$$A_e = W_e\, t \quad (7)$$

The width of the strut in terms of the height of the panel h and panel length l can be expressed as:

$$W_e = 0.175(\lambda h)^{-0.4}\sqrt{h^2 + l^2} \quad (8)$$

Where, the value of λ can be calculated as:

$$\lambda = \sqrt[4]{\frac{E_m t \sin(2\theta)}{4E_c I_c H_w}} \quad (9)$$

Where, E_c and E_m respectively denote the elastic moduli of the column and the masonry wall, θ is the angle defining diagonal strut inclination which is the angle between the diagonal of the panel and the horizontal plane, I_c is the moment of inertia of the column and H_w is the height of the infill wall.

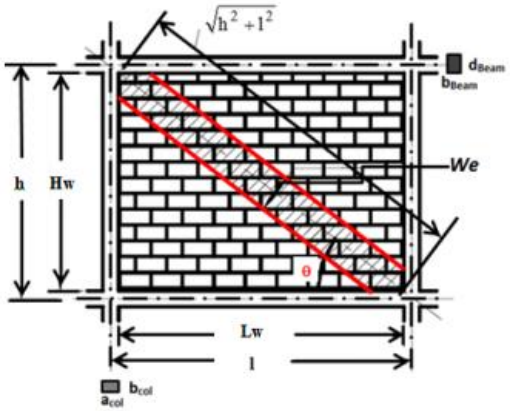

Figure 7: Equivalent strut model for masonry infill walls in frame structures

III. Modelling and Analysis

3.1 General

In this paper, all analysis and design of members are carried out using commercial software و ETABS 17. Fifty different models of 2D frames have been created and grouped into ten different groups depending on the height, percentage of infill and performance level of the frame. For each height group, frames were further grouped based on their performance levels. These levels were achieved by varying reinforcement ratios in the structural members between two limits, namely lower and upper limits. Upper limits refer to the required reinforcement ratios needed to achieve the best performance of the frames, whilst lower limits refer to the least performance. Upper limits are achieved by designing frames conforming the ECP-201 and ECP-203 FBD design method, satisfying the corresponding lateral and vertical load combinations, whilst lower limits are achieved by designing frames under vertical loads only.

Groups (A, D, G and I)* are designed conforming the ECP-201 FBD design method, and are assigned the (*) notation to be distinguished as code-complaint designed (CCD) models. According to ECP-201 seismic provisions, which follows the guidelines of Eurocode 8 (CEN, 2004), the value of horizontal design spectrum is set to a minimum value of $0.2*a_g*\gamma_1$, where a_g is the design ground acceleration and γ_1 is structure's importance factor. Consequently, to achieve different performance levels for structures with longer time periods, this limitation of horizontal design spectrum has to be neglected. The remaining groups will be categorized as groups (B, E and H) for life safety and groups (C and F) for collapse prevention.

Groups (C, F, H and J) were first designed under vertical loads only. The two tallest frame groups, groups (C and F) showed least performance, collapse prevention (CP); hence were redesigned for seismicity with no spectral limitation, to enhance the performance level and achieve two new groups, groups (B and E), that show higher performance level namely, life safety (LS). Group (H) showed intermediate life safety (LS) performance directly when designed under vertical loading; while the shortest group of all, Group (J), showed immediate occupancy (IO) performance under vertical loading.

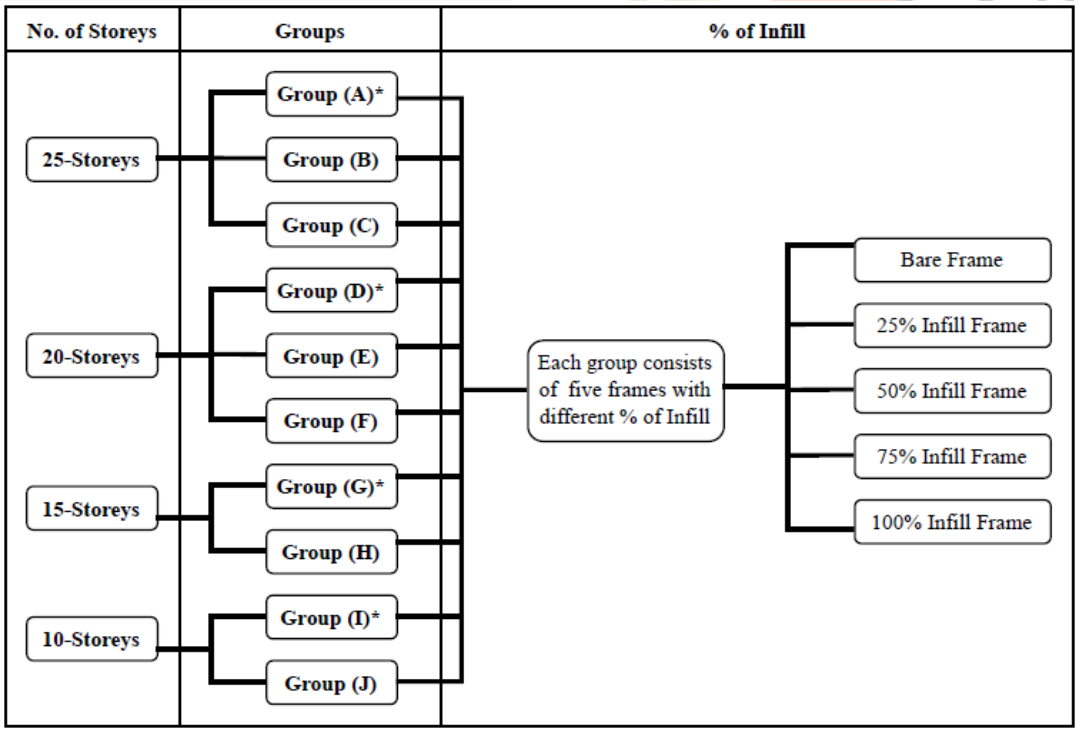

Figure 8: Structural models group classification

In this paper, infill irregularities are avoided in all forms to avoid the adverse effects that may arise such as short-column and soft storey effects. On the other hand, infill percentages are referred to as the number of bays of the bare frame being filled with the URM infills.

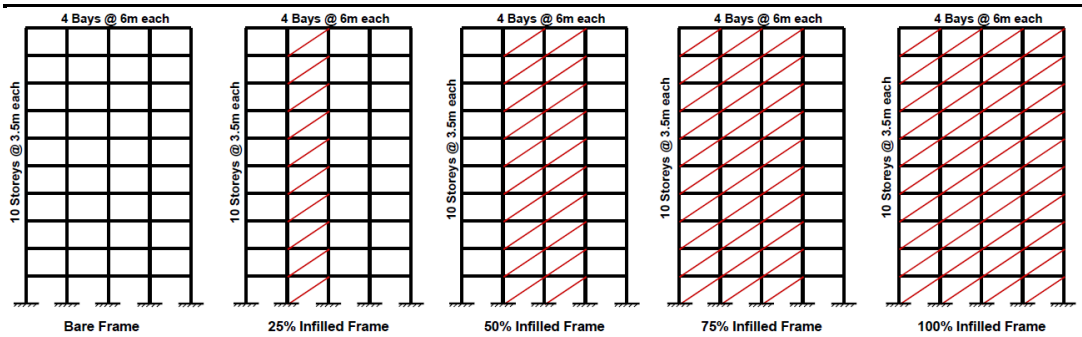

Figure 9: Example of infill distribution in 10-Storey frame

All frames in the scope of study are considered as an intermediate frame; hence loadings subjected on the frames are an imposition from adjacent bays on both sides.

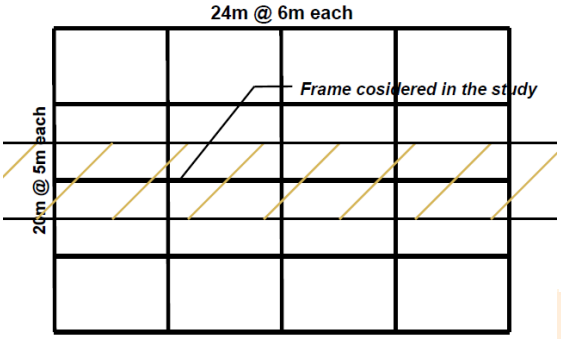

Figure 10: Typical plan for the studied frame

3.2 Concrete Dimensions and Reinforcement Ratios

For each height group, concrete dimensions for columns and beams are kept the same. Concrete dimensions are chosen based on designing the bare frames of the CCD models, satisfying the ECP-203 load combinations, drift control and deflection of beams. Different performance levels of frames are later achieved by varying the reinforcement ratios of horizontal members, beams, only, based on which performance group the models follow.

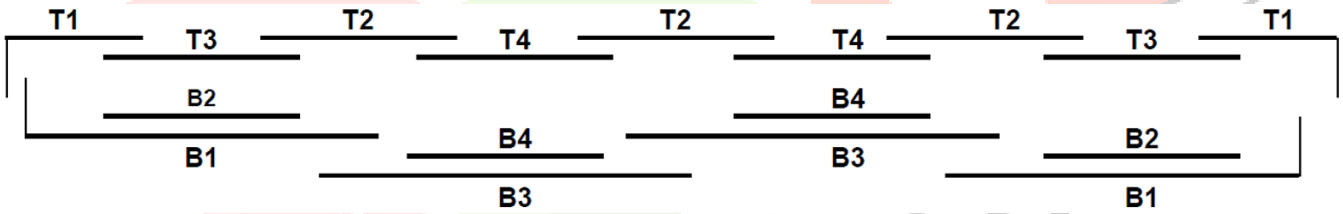

Figure 11: Beams reinforcement notations

Table 3: Concrete Sections and Reinforcement Ratios

o. toreys	tructure leight (m)	roup	Storey Level for Columns	Columns Dimensions (mm) and Reinforcement	Beams Dimensions (mm)	Beams Reinforcement							
						Storey Level for Beams	T1	T2	B1	B2	B3	B4	T3	T4
25- Storeys	87.5	Group A)*	20th to 25th	00x500 2T16 1.00%)	250x850	25th	5T12	5T12	3T12	2T12	3T12	2T12	2T12	2T12
						22nd to 24th	5T18	5T18	4T12	2T12	4T12	2T12	2T12	2T12
						19th to 21th	5T20	5T20	4T16		4T16		2T12	2T12
			14th to 19th	00x600 0T16 1.10%)		16th to 18th	4T25	4T25	5T18		5T18		3T12	3T12
						12th to 15th	3T32	3T32	5T20		5T20		3T12	3T12
						2th to 11th	4T32	4T32	4T25		4T25		4T12	4T12
						1st	4T25	4T25	4T22		4T22		4T12	4T12
		Group B)	8th to 13th	50x650 0T22 1.80%)		25th	4T12	4T12	4T12	3T12	4T12	2T12	2T12	2T12
						18th to 24th	5T18	5T12	4T12	2T12	4T12	2T12	2T12	2T12
						11th to 17th	4T20	4T16	4T12	2T12	4T12	2T12	2T12	2T12
						3rd to 10th	4T18	4T16	4T12	2T12	3T12	2T12	2T12	2T12
						1st to 2nd	4T16	4T16	4T12	2T12	4T12	2T12	2T12	2T12
		Group C)	1st to 7th	50x750 4T25 2.10%)		25th	4T12	4T12	4T12	3T12	3T12	2T12	2T12	2T12
						14th to 24th	5T18	5T12	4T12	2T12	3T12	2T12	2T12	2T12
						8th to 13th	5T16	5T12	4T12	2T12	4T12	2T12	2T12	2T12
						1st to 7th	4T16	4T16	3T12	2T12	3T12	2T12	2T12	2T12
20- Storeys	70	Group D)*	17th to 20th	450x450 T22 1.50%)	250x750	20th	5T12	5T12	3T12	2T12	3T12	2T12	2T12	2T12
						17th to 19th	4T18	4T18	5T12	3T12	4T12	2T12	2T12	2T12
						15th to 16th	4T20	4T18	4T16		4T16		2T12	2T12
						13th to 14th	4T25	4T20	4T18		4T18		3T12	3T12
						11th to 12th	4T25	4T22	4T20		4T20		3T12	3T12
			14th to 16th	500x500 2T20 1.50%)		9th to 10th	4T25	4T25	4T22		4T22		4T12	4T12
						2nd to 8th	3T32	3T32	4T25		4T25		4T12	4T12
						1st	4T22	4T22	4T20		4T20		3T12	3T12
		Group E)	8th to 13th	600x600 0T18 1.40%)		20th	5T12	5T12	3T12	2T12	3T12	2T12	2T12	2T12
						10th to 19th	4T18	4T16	4T12	2T12	4T12	2T12	2T12	2T12
						2nd to 9th	4T18	4T18	4T12	2T12	4T12	2T12	2T12	2T12
						1st	4T16	4T16	3T12	2T12	3T12	2T12	2T12	2T12
		Group F)	1st to 7th	700x700 4T22 1.90%)		20th	5T12	5T12	3T12	2T12	3T12	2T12	2T12	2T12
						10th to 19th	5T16	5T12	4T12	2T12	3T12	2T12	2T12	2T12
						3rd to 9th	4T16	4T16	3T12	2T12	3T12	2T12	2T12	2T12
						1st to 2nd	3T16	3T16	3T12	2T12	3T12	2T12	2T12	2T12
15- Storeys	52.5	Group G)*	11th to 15th	450x450 T18 1.00%)	250x700	15th	5T12	5T12	3T12	2T12	3T12	2T12	2T12	2T12
						13th to 14th	4T18	4T16	4T12	2T12	3T12	2T12	2T12	2T12
						11th to 12th	4T20	4T18	4T12	2T12	4T12	2T12	2T12	2T12
						9th to 10th	4T22	4T20	4T16		4T16		2T12	2T12
			8th to 10th	550x550 6T16 1.10%)		7th to 8th	4T22	4T22	4T18		4T18		2T12	2T12
						2nd to 6th	4T25	4T22	4T20		4T20		2T12	2T12
						1st	4T20	4T20	4T18		4T18		2T12	2T12
		Group H)	5th to 7th	600x600 0T16 1.10%)		15th	5T12	5T12	3T12	3T12	3T12	3T12	2T12	2T12
						6th to 14th	5T16	5T12	3T12	3T12	3T12	3T12	2T12	2T12
						3rd to 5th	4T16	4T16	3T12	3T12	3T12	3T12	2T12	2T12
			1st to 4th	650x650 0T18 1.20%)		1st to 2nd	3T16	3T16	3T12	3T12	3T12	3T12	2T12	2T12
No. of Storeys	**Structure Height (m)**	**Group**	**Storey Level for Columns**	**Columns Dimensions (mm) and Reinforcement**	**Beams Dimensions (mm)**	**Beams Reinforcement**								
						Storey Level for Beams	**T1**	**T2**	**B1**	**B2**	**B3**	**B4**	**T3**	**T4**
10- Storeys	35	Group (I)*	9th to 10th	400x400 T18 1.27%)	250x600	10th	4T12	4T12	4T12	3T12	4T12	3T12	2T12	2T12
						8th to 9th	4T18	4T18	4T12	3T12	3T12	3T12	2T12	2T12
			5th to 8th	450x450 T18 1.00%)		6th to 7th	4T22	4T20	4T16		4T12		2T12	2T12
						2nd to 5th	4T25	4T25	4T16		4T16		2T12	2T12
			3rd to 4th	500x500 2T16 1.00%)		1st	4T22	4T22	4T16		4T16		2T12	2T12
		Group (J)				10th	4T12	4T12	4T12	3T12	4T12	3T12	2T12	2T12
			1st to 2nd	550x550 6T16 1.10%)		9th	4T16	4T16	3T12	3T12	3T12	3T12	2T12	2T12
						1st to 8th	4T18	4T18	3T12	3T12	3T12	3T12	2T12	2T12

3.3 Material Properties

All materials used comply with the Egyptian standard specifications ECP-203 and ECP-204.

Concrete:

- Compressive Cube Concrete Strength (F_{cu})= 35 MPA
- Density of reinforced concrete (γ_c)= 2.5 ton/m^3
- Modulus of Elasticity (E_c)= 26030.75 MPA

Reinforcement: High strength steel reinforcement is used.

- Longitudinal bars: F_y= 420 MPA, F_u= 525 MPA
- Confinement tie: F_y= 400 MPA, F_u= 500 MPA

Masonry: Red clay bricks are used.

- Density of masonry infill (γ_m)= 1.8 ton/m^3
- F_{cu}= 15MPA (Single unit)
- F'$_m$= 4.8 MPA (Brick wall)
- F_{design}= 0.85*F'$_m$= 4.08 MPA
- Modulus of Elasticity (E_m)= 700* F'$_m$= 3360 MPA
- Shear Modulus (G_{URM})= 0.4*E_m=1344 MPA
- Dimension of single brick= length* thickness *height= 240mm*112mm*70mm

3.4 Vertical Design Loads

All frames in the scope of study are considered as an intermediate frame; hence loadings subjected on the frames are an imposition from adjacent bays on both sides.

- 15cm thickness reinforced slab= 0.375 ton/m^2
- 4cm thickness marble floor cover= 0.1 ton/m^2
- Live load for office buildings= 0.25 ton/m^2
- 1.8 ton/m^3 density infill walls taken as line loads on beams= 0.5 ton/m'

3.5 Seismic Loads

Seismic and soil parameters are assumed according to the ECP-201 recommendations, as follows,

- Soil Type: D
- Seismic Zone: 5B
- Importance Factor: 1.0
- Response Spectrum Type: Type 1
- Ground Acceleration (a_g): 0.3g

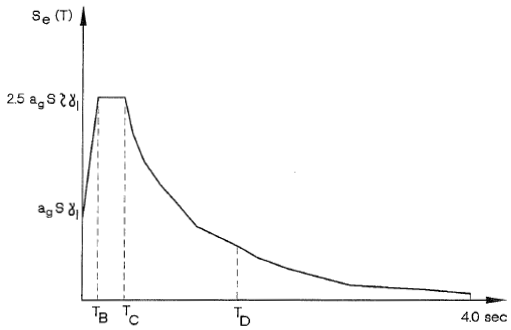

Figure 12: Type 1 Response Spectrum

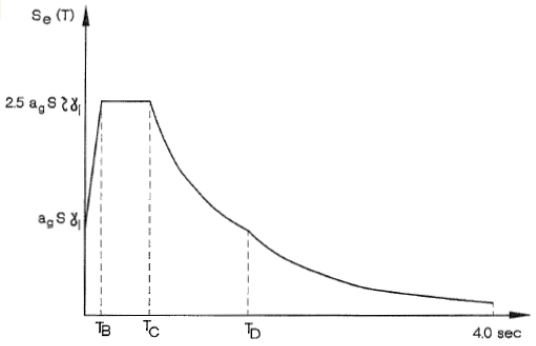

Figure 13: Type 2 Response Spectrum

Type 2 Response spectrum is used only for coastal regions on the Mediterranean Sea. The region considered in this paper is south Sinai Peninsula on the Red Sea, seismic zone 5B.

IV. Results and Discussions

As mentioned earlier pushover analysis is conducted on different models with different heights and infills percentages to achieve force-displacement curves. In this section a comparative study is displayed and discussed to clarify and compare the behavior of the different structures for better understanding of infill contribution to the frame structures with different heights.

4.1 Infills Contribution

Simple Lateral Mechanism Analysis, namely (SLaMA), is an analytical method provided by the New Zealand Society for Earthquake Engineering (NZSEE 2017) to assess and capture the behavior of RC structures. A study was published by Roberto Gentile (2019), proposing a comprehensive SLaMA method for infilled frames, which considers the influence of the infills on the global force–displacement curve without any numerical algorithm. The extended SLaMA method is based on the possibility to separately calculate the base shear contributions of the bare frame, $V_{B,RC}$, and the infills, $V_{B,INF}$, in turn based on the global equilibrium considerations.

$$V_{B,RC} = V_{B,TOT} - V_{B,INF} \quad (10)$$

The procedure on how to separate the $V_{B,RC}$ and $V_{B,INF}$ from the total base shear of the infilled frame, $V_{B,TOT}$, depends on the contribution of infills and bare frame to the global response of the structure is comprehensively studied by Roberto Gentile (2019) ; and which is not the scope of this paper. Instead, the direct contribution of infill is simply calculated as per (equation 10).

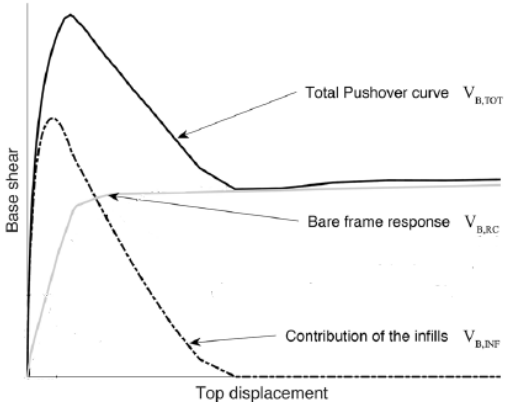

Figure 14: Disaggregation of the frame and infills contributions within a single pushover

To understand the significance of infill contribution on the behavior of the structure and its effect on P-factor, results of infill contribution achieved for each group is defined in terms of energy absorption /dissipation by both the infill and the members of the frame structure itself. The ratio of energy absorption by the infill and the structure is later used to conclude infill effects on the performance of the structure as will be elaborated in the paper. Energy absorption is achieved by extracting the area underneath the push over curves shown in the upcoming figures.

4.1.1 25-Storey Frames Models Results

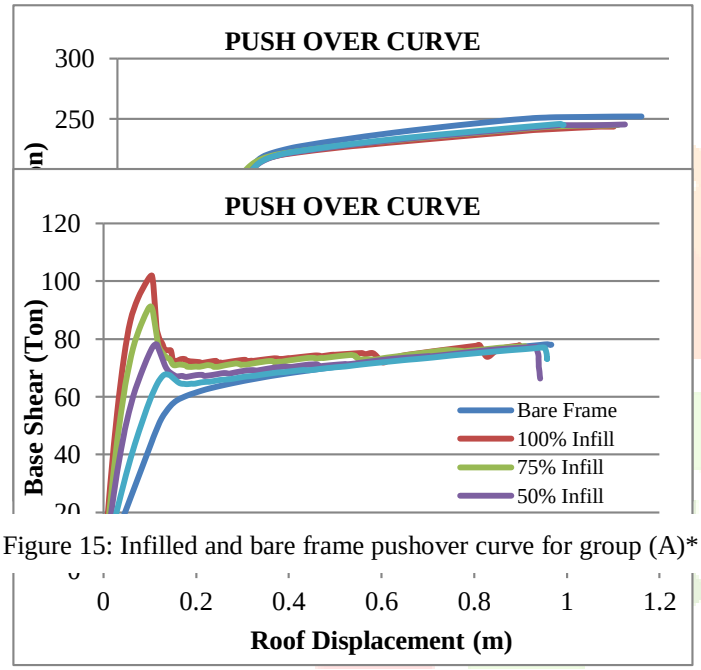

Figure 15: Infilled and bare frame pushover curve for group (A)*

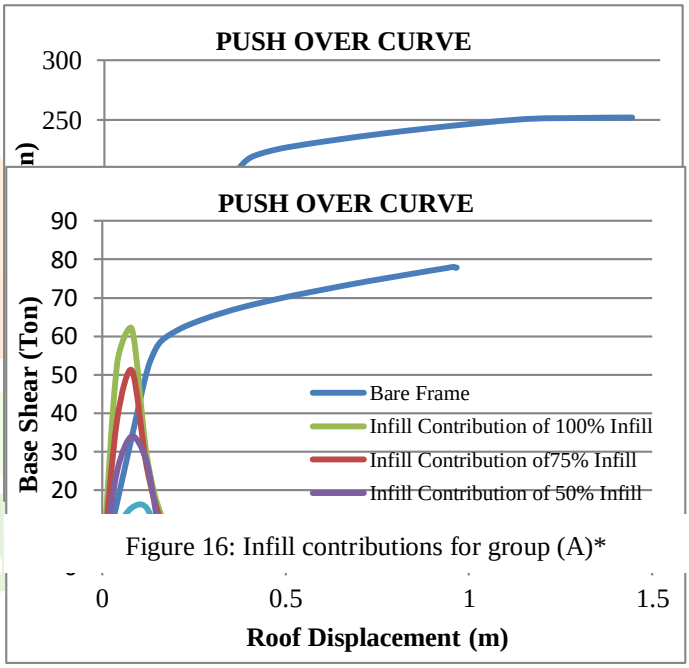

Figure 16: Infill contributions for group (A)*

Figure 17: Infilled and bare frame pushover curve for group (B)

Figure 18: Infill contributions for group (B)

frames

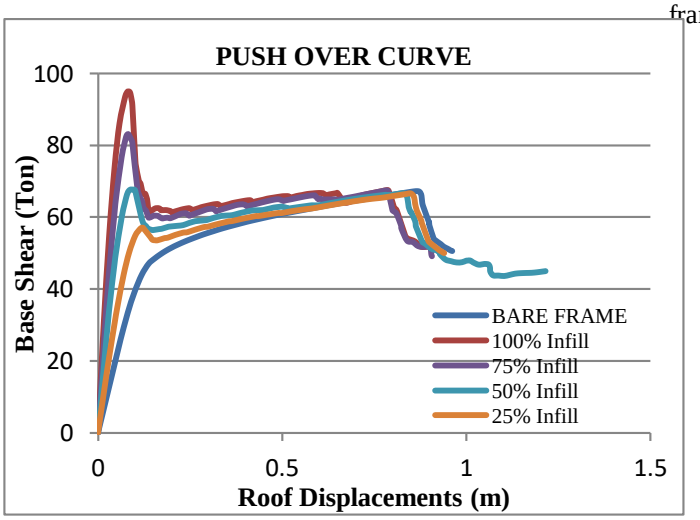

Figure 19: Infilled and bare frame pushover curve for group (C)

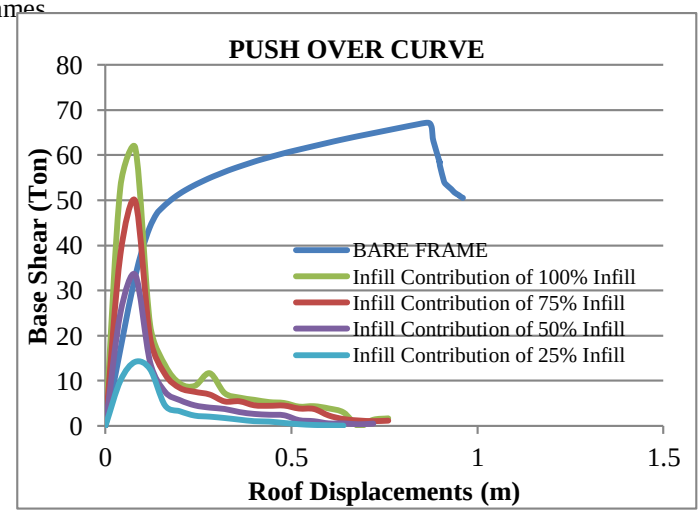

Figure 20: Infill contributions for group (C)

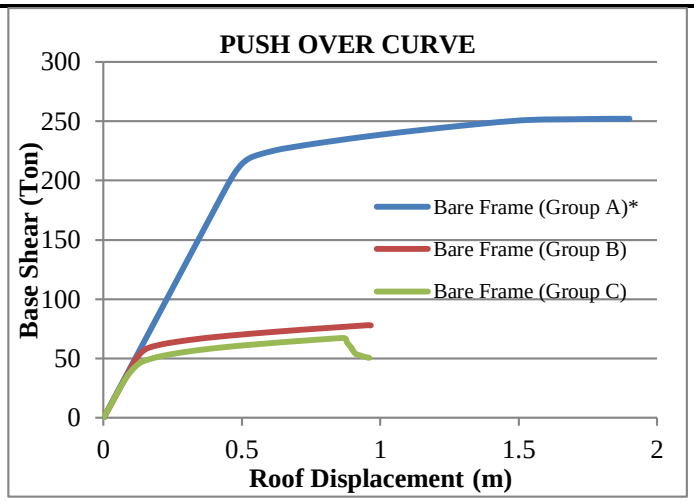

4.1.1.1 Conclusion and Discussion for 25-Storey Frames

Table 4: Energy absorption for 25-storey frames

Groups	Infill Percentages	Absorbed Energy by Bare Frame (kN)	Absorbed Energy by Infill (kN)	Ratio of Absorbed Energy by Infill to Bare Frame (%)
Group (A)*	25% Infill	3927.00	37.00	0.94
	50% Infill		70.00	1.78
	75% Infill		125.00	3.18
	100% Infill		135.00	3.44
Group (B)	25% Infill	623.00	22.80	3.66
	50% Infill		48.30	7.75
	75% Infill		71.40	11.46
	100% Infill		87.50	14.04
Group (C)	25% Infill	527.00	21.80	4.14
	50% Infill		44.70	8.48
	75% Infill		71.70	13.61
	100% Infill		90.00	17.08

First, results in the previous table shows that as infill percentage in the frame increases as does the total energy absorbed by the infill, which is an expected conclusion as more infill tends to crack, hence more dissipate energy. Moreover, results suggest that for CCD models, infills would absorb less energy in terms of ratio to the energy absorbed by the bare frame; while for less ductility detailed frames (less performing frames), infills would absorb much more energy in terms of ratio. This can be as a result to the fact that CCD models are designed to follow more conservative drift limits, explained in section 4.2.5, hence show less deformity; leaving infills less prone to accept more energy in terms of ratio during a seismic event; hence, sustain less damage at earlier stages of the pushover analysis. This conclusion could explain the reason why infills with CCD models show higher contribution to the P-factor and to global ductility of the frames as compared to less performing frames; this would be elaborated in the later sections.

4.1.2 20-Storey Frames Models Results

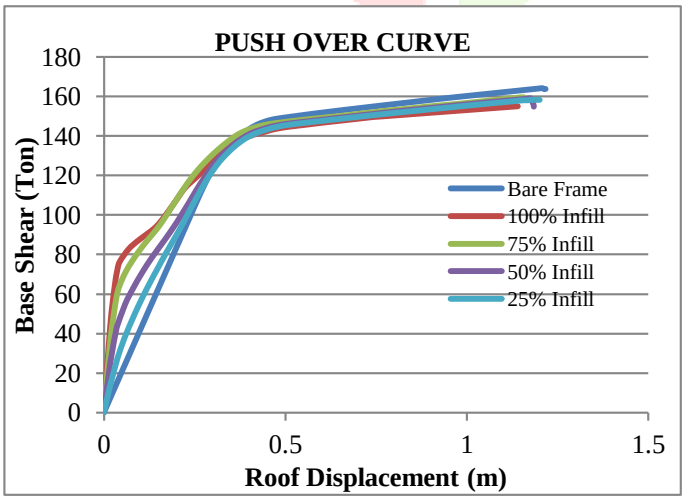

Figure 22: Infilled and bare frame pushover curve for group (D)*

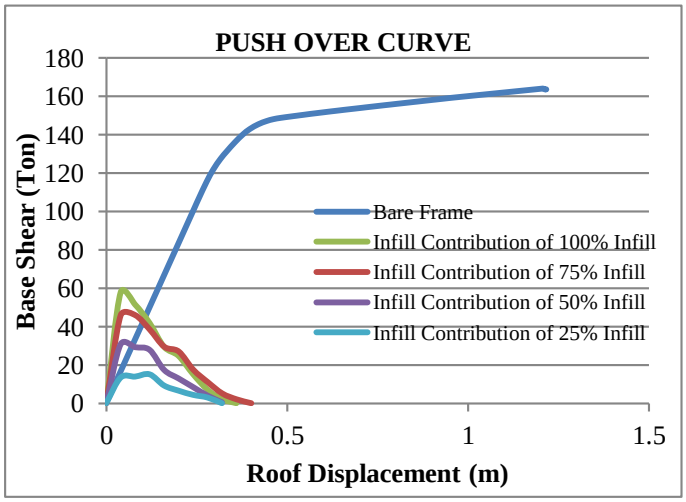

Figure 23: Infill contributions for group (D)*

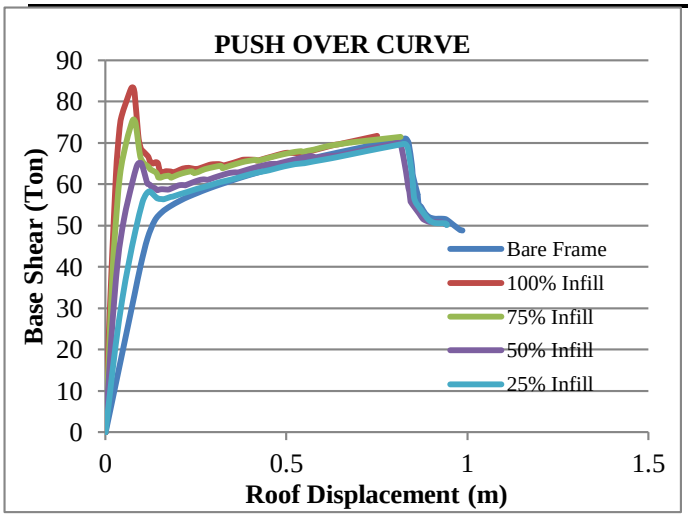

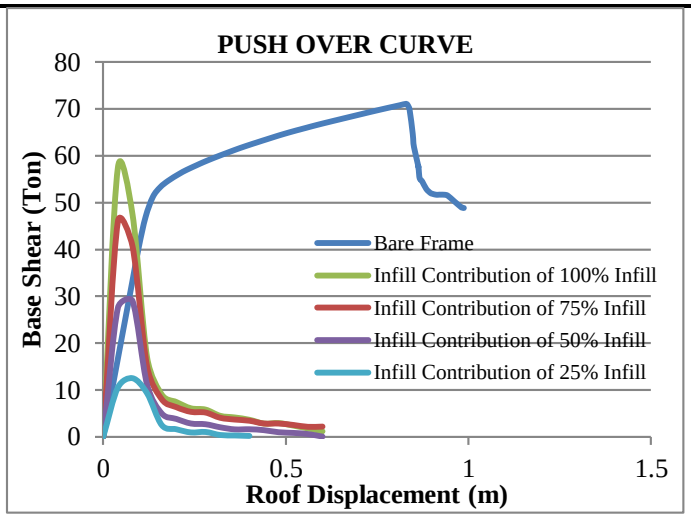

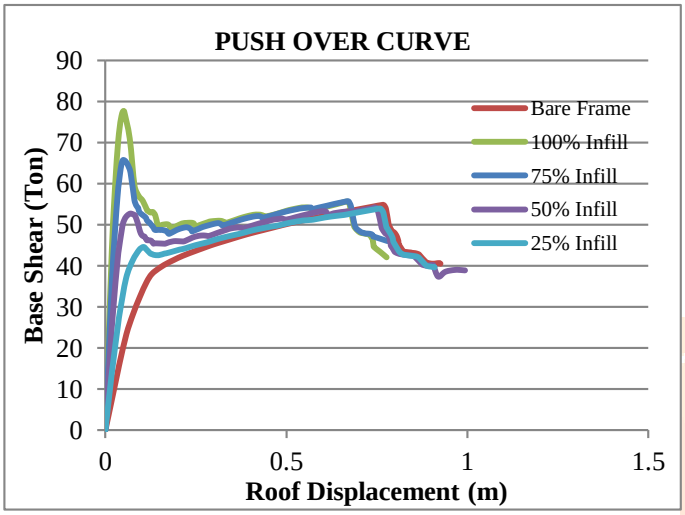

F

Figure 26: Infilled and bare frame pushover curve for group (F)

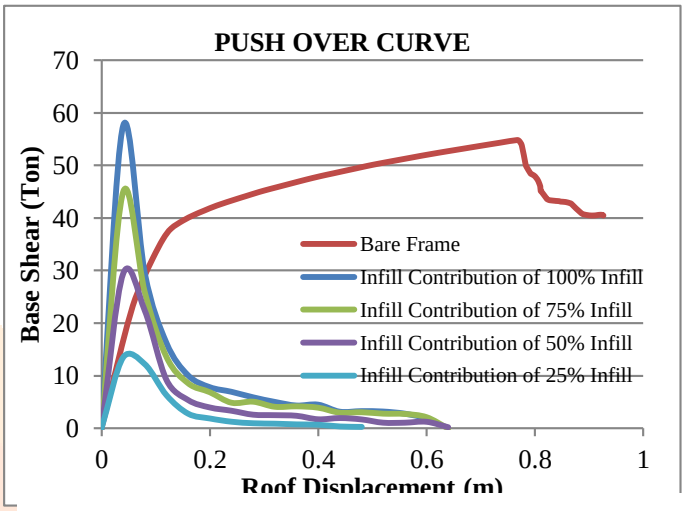

Figure 25: Infill contributions for group (E)

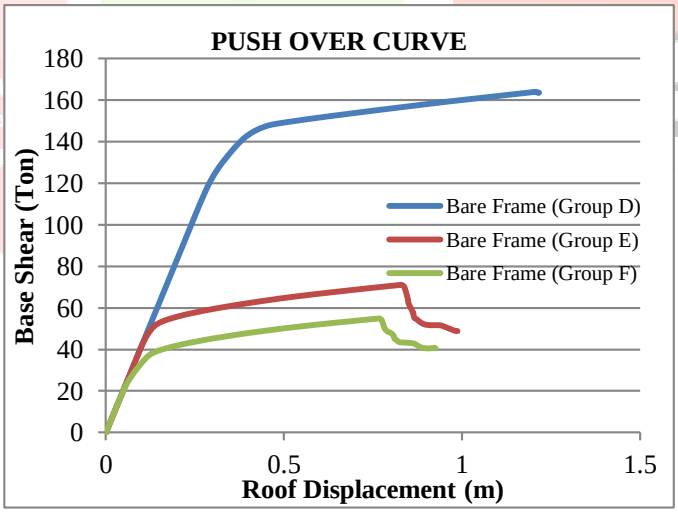

Figure 28: Pushover curve comparison for 20-storey height bare frames

4.1.2.1 Conclusion and Discussion for 20-Storey Frames

Table 5: Energy absorption for 20-storey frames

Groups	Infill Percentages	Absorbed Energy by Bare Frame (kN)	Absorbed Energy by Infill (kN)	Ratio of Absorbed Energy by Infill to Bare Frame (%)
Group (D)*	25% Infill	1595.00	26.40	1.66
	50% Infill		52.60	3.30
	75% Infill		89.00	5.58
	100% Infill		91.80	5.76
Group (E)	25% Infill	564.40	15.50	2.75
	50% Infill		36.20	6.41
	75% Infill		59.50	10.54
	100% Infill		69.00	12.23
Group (F)	25% Infill	408.00	16.70	4.09
	50% Infill		36.10	8.85
	75% Infill		54.40	13.33
	100% Infill		65.00	15.93

The table above suggests similar conclusions as explained in section 4.1.1.1.

4.1.3 15-Storey Frames Models Results

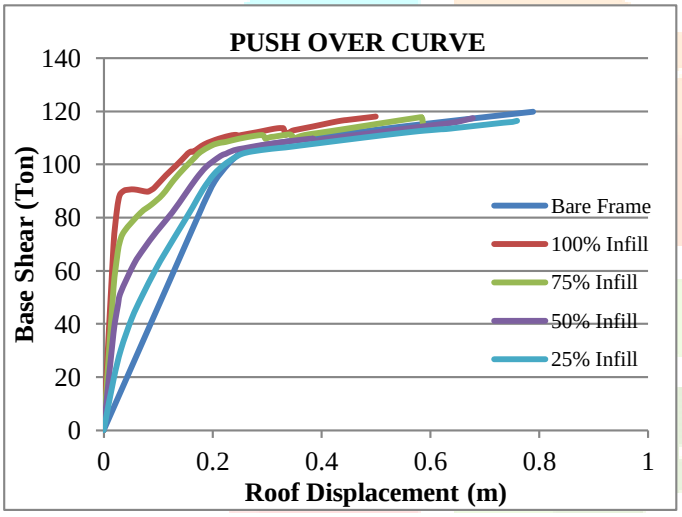

Figure 29: Infilled and bare frame pushover curve for group (G)*

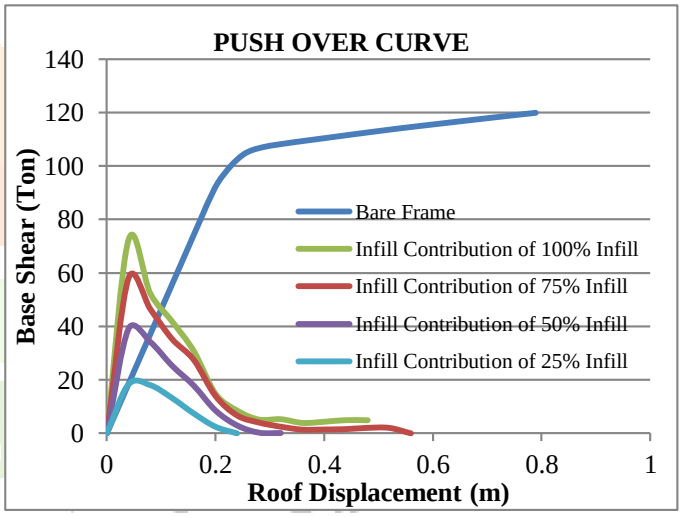

Figure 30: Infill contributions for group (G)*

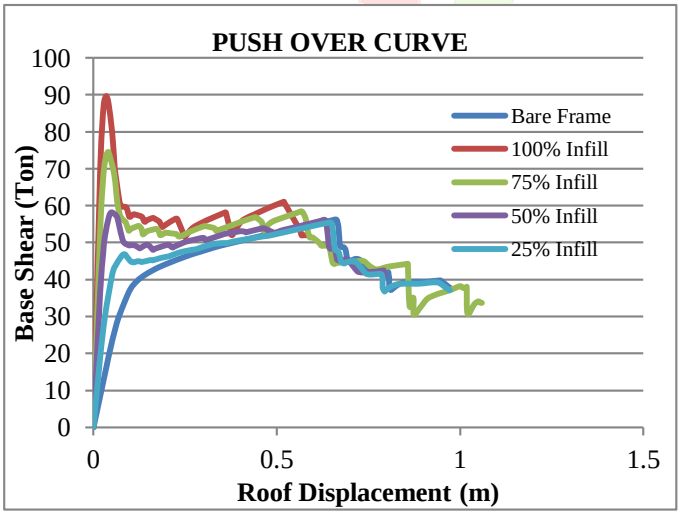

Figure 31: Infilled and bare frame pushover curve for group (H)

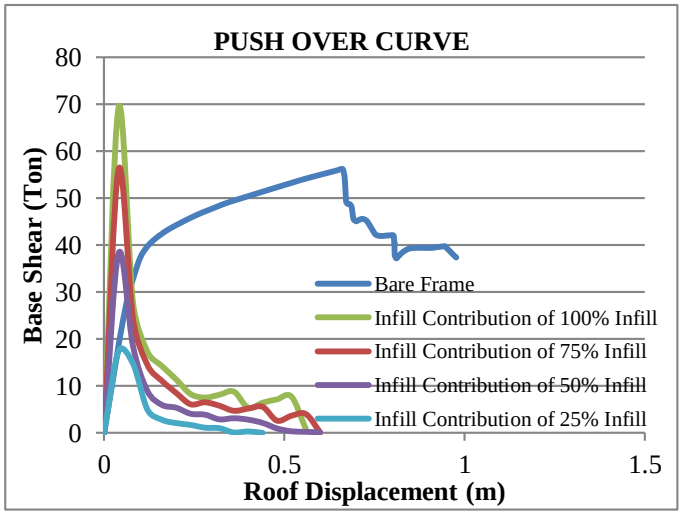

Figure 32: Infill contributions for group (H)

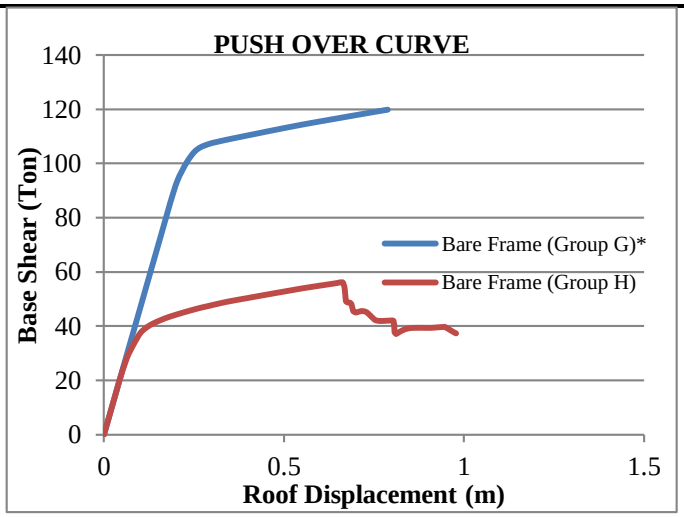

Figure 33: Pushover curve comparison for 15-storey height bare frames

4.1.3.1 Conclusion and Discussion for 15-Storey Frames

Table 6: Energy absorption for 15-storey frames

Groups	Infill Percentages	Absorbed Energy by Bare Frame (kN)	Absorbed Energy by Infill (kN)	Ratio of Absorbed Energy by Infill to Bare Frame (%)
Group (G)*	25% Infill	753.00	23.90	3.17
	50% Infill		51.10	6.79
	75% Infill		81.20	10.78
	100% Infill		98.70	13.11
Group (H)	25% Infill	429.20	18.40	4.29
	50% Infill		38.50	8.97
	75% Infill		63.00	14.68
	100% Infill		79.50	18.52

The table above suggests similar conclusions as explained in section 4.1.1.1.

4.1.4 10-Storey Frames Models Results

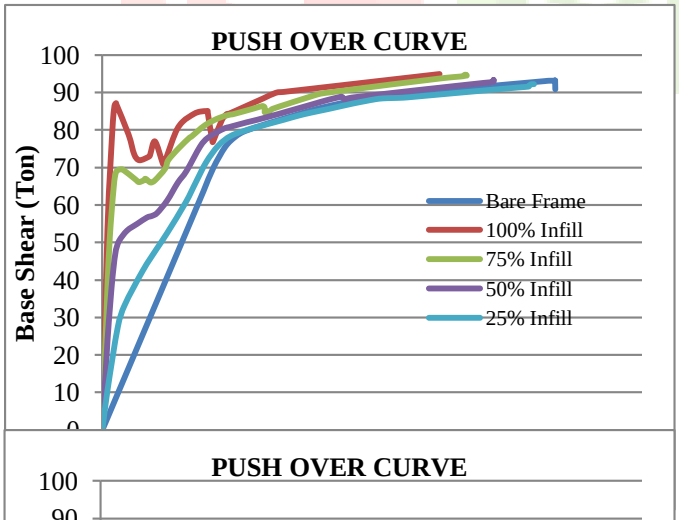

Figure 34: Infilled and bare frame pushover curve for group (I)*

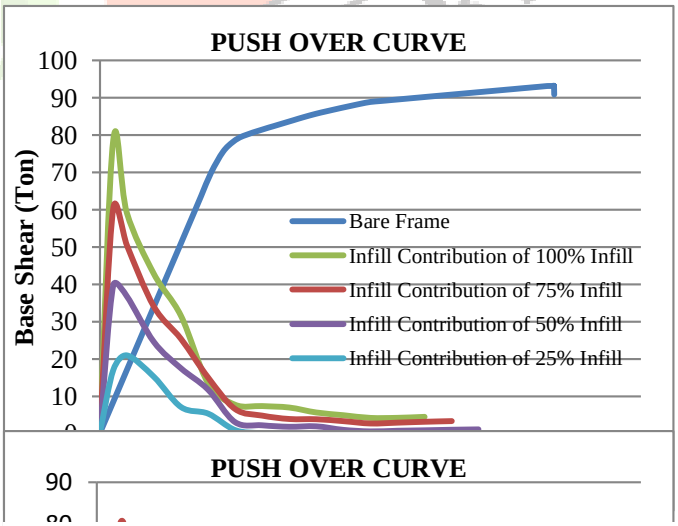

Figure 35: Infill contributions for group (I)*

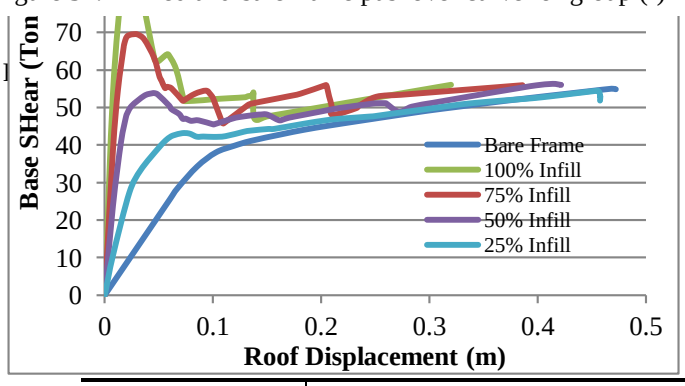

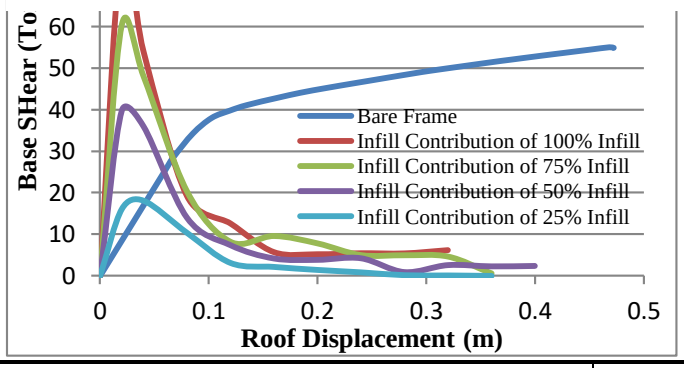

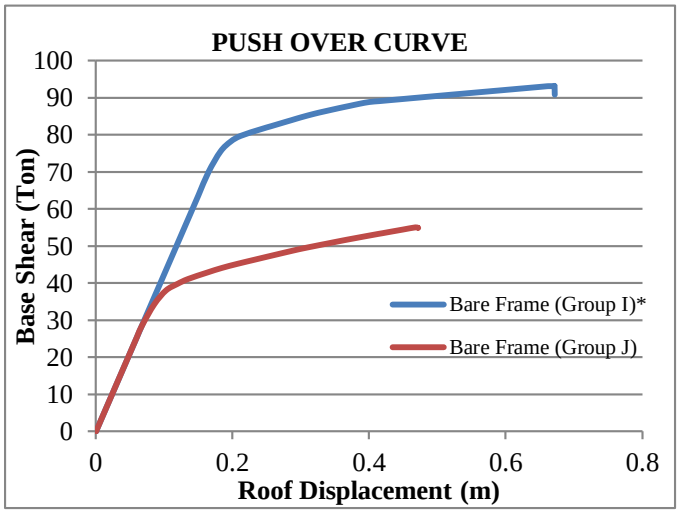

Figure 38: Pushover curve comparison for 10-storey height bare frames

4.1.4.1 Conclusion and Discussion for 10-Storey Frames

Table 7: Energy absorption for 10-storey frames

Groups	Infill Percentages	Absorbed Energy by Bare Frame (kN)	Absorbed Energy by Infill (kN)	Ratio of Absorbed Energy by Infill to Bare Frame (%)
Group (I)*	25% Infill	500.00	21.00	4.20
	50% Infill		46.00	9.20
	75% Infill		70.00	14.00
	100% Infill		85.90	17.18
Group (J)	25% Infill	199.40	15.80	7.92
	50% Infill		35.00	17.55
	75% Infill		50.80	25.48
	100% Infill		54.60	27.38

The table above suggests similar conclusions as explained in section 4.1.1.1.

4.2 Effects of Infills on Performance of Structures

In this paper, the improved version of the Capacity Spectrum Method, provided by FEMA-440, is used in the study to obtain the performance point of the respective structures; and of which was further described in the methodology section (2.1). The acceleration-displacement response spectrum curve (ADRS) is developed from the pushover curve, force-displacement curve, and the performance point is achieved by graphical intersection of the demand and ADRS curves.

As shown previously, pushover curves for infilled frames show a lot of deformities as compared to the bare frame analysis, as more URM panels are damaged with the increasing steps of the pushover analysis; resulting in difficulties in reading and determining the P factor components that was comprehensively described in the methodology section (2.2). Therefore, a conservative assumption allowing for the uncertainties that could arise owing to the possible existence of pre-cracks in infills and/or the presence of construction flaws in real life practicality of the URM panels. Thus the initial stiffness of infilled frames, $k_{i,infill}$, was not considered as the prominent stiffness value used in calculating the P factor, instead, an effective initial stiffness, $k_{effect,infill}$, is considered. The method used to obtain the $k_{effect,infill}$ of the infilled frame is briefly described in the figure below.

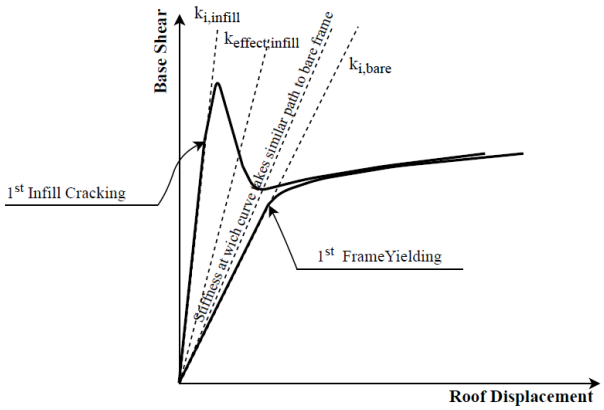

Figure 39: Assumed procedure for calculating effective initial stiffness for infilled frames

4.2.1 25-Storey Frames Models Results

Table 8: Performance points and performance levels of 25-storey height frames (* is for $k_{i.bare}$)

No. of Stories	Group	% of Infill	$k_{effect.infill}$ (ton/m)	$k_{effect.infill}/k_{i.bare}$	Performance Level	P- Factor	Increase in P-Factor (%)
25-Stories	Group (A)*	Bare Frame	424*		IO	5.56	0.00
		25% Infill	586.4	1.38	IO	7.23	30.08
		50% Infill	776	1.83	IO	9.47	70.30
		75% Infill	936.26	2.20	IO	11.21	101.57
		100% Infill	1016.7	2.39	IO	12.07	117.07
	Group (B)	Bare Frame	424*		LS (64 LS Hinges)	13.64	0.00
		25% Infill	484.9	1.14	LS (40 LS Hinges)	15.09	10.60
		50% Infill	518.8	1.22	LS (36 LS Hinges)	15.82	15.98
		75% Infill	615.1	1.45	LS (32 LS Hinges)	18.21	33.54
		100% Infill	740.9	1.74	LS (9 LS Hinges)	21.65	58.75
	Group (C)	Bare Frame	424*		CP (9 CP Hinges)	14.82	0.00
		25% Infill	482.6	1.13	LS (75 LS Hinges)	15.90	7.25
		50% Infill	513.1	1.21	LS (73 LS Hinges)	16.41	10.71
		75% Infill	601.8	1.41	LS (65 LS Hinges)	18.58	25.37
		100% Infill	710.5	1.67	LS (46 LS Hinges)	21.68	46.26

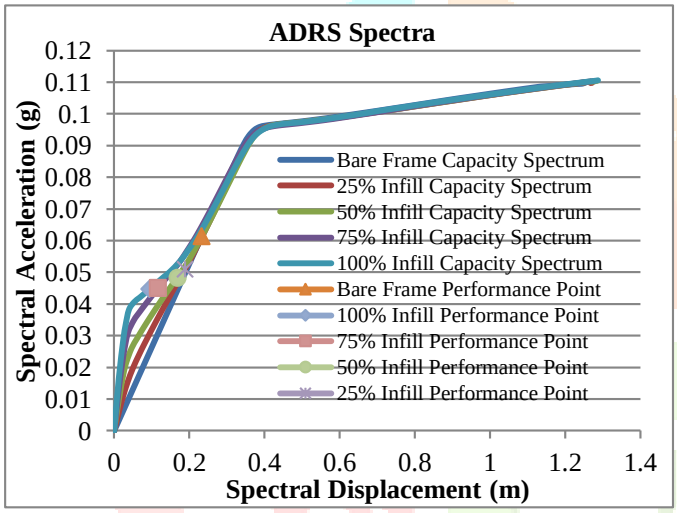

Figure 40: Performance points illustration for group (A)*

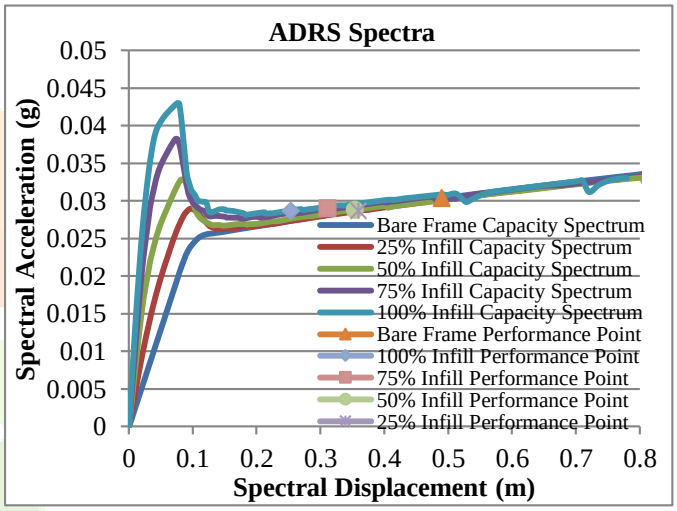

Figure 41: Performance points illustration for group (B)

Figure 42: Performance points illustration for group (C)

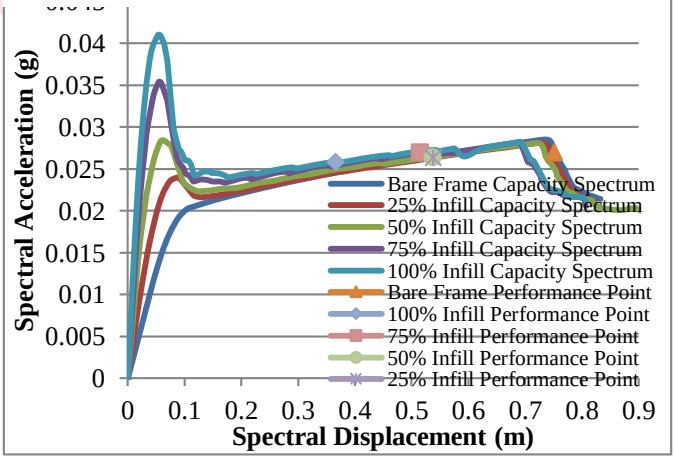

4.2.2 20-Storey Frames Models Results

Table 9: Performance points and performance levels of 20-storey height frames (* is for $k_{i.bare}$)

No. of Stories	Group	% of Infill	$k_{effect.infill}$ (ton/m)	$k_{effect.infill}/k_{i.bare}$	Performance Level	P- Factor	Increase in P-Factor (%)
20-Stories	Group (D)*	Bare Frame	417.4*		IO	4.50	0.00
		25% Infill	694.3	1.66	IO	7.06	56.84
		50% Infill	823.8	1.97	IO	8.17	81.45
		75% Infill	907.4	2.17	IO	8.93	98.32
		100% Infill	1013.1	2.42	IO	9.79	117.41
	Group (E)	Bare Frame	417.4*		LS (38 LS Hinges)	13.71	0.00
		25% Infill	488.1	1.16	LS (13 LS Hinges)	15.02	9.53
		50% Infill	519.3	1.24	LS (7 LS Hinges)	15.61	13.81
		75% Infill	621.7	1.48	IO	18.13	32.21
		100% Infill	787.9	1.88	IO	21.14	54.19
	Group (F)	Bare Frame	417.4*		CP (5 CP Hinges)	14.42	0.00
		25% Infill	457.6	1.09	LS (71 LS Hinges)	15.58	8.05
		50% Infill	478.8	1.14	LS (65 LS Hinges)	15.96	10.68
		75% Infill	557	1.33	LS (57 LS Hinges)	18.10	25.55
		100% Infill	654.1	1.56	LS (41 LS Hinges)	20.71	43.66

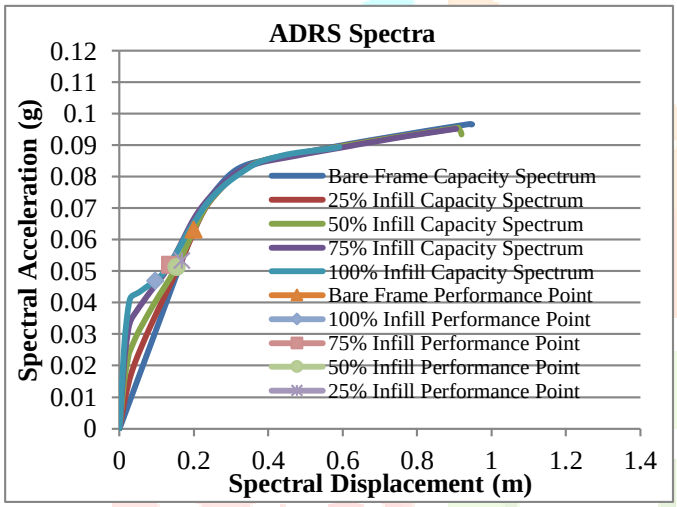

Figure 43: Performance points illustration for group (D)*

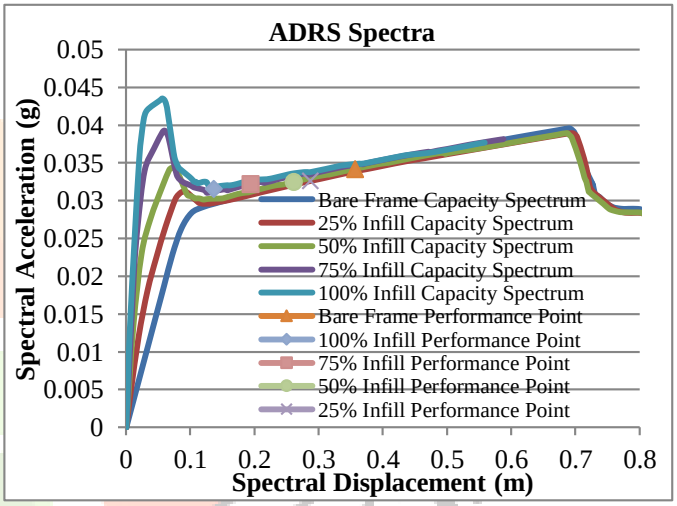

Figure 44: Performance points illustration for group (E)

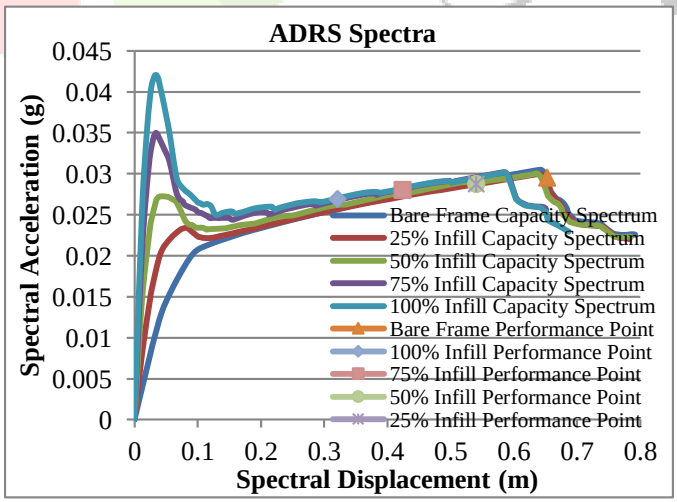

Figure 45: Performance points illustration for group (F)

4.2.3 15-Storey Frames Models Results

Table 10: Performance points and performance levels of 15-storey height frames (* is for $k_{i.bare}$)

No. of Stories	Group	% of Infill	$k_{effect.infill}$ (ton/m)	$k_{effect.infill}/k_{i.bare}$	Performance Level	P- Factor	Increase in P-Factor (%)
15-Stories	Group (G)*	Bare Frame	464.6*		IO	4.28	0.00
		25% Infill	718.1	1.54	IO	6.30	47.25
		50% Infill	1011.2	2.17	IO	7.84	83.29
		75% Infill	1294.5	2.78	IO	8.72	103.83
		100% Infill	1593.8	3.433	IO	9.22	115.59
	Group (H)	Bare Frame	464.6*		LS (11 LS Hinges)	13.68	0.00
		25% Infill	480.9	1.03	IO	15.00	9.61
		50% Infill	511.8	1.10	IO	15.84	15.77
		75% Infill	584.2	1.25	IO	17.80	30.11
		100% Infill	717.6	1.54	IO	19.99	46.09

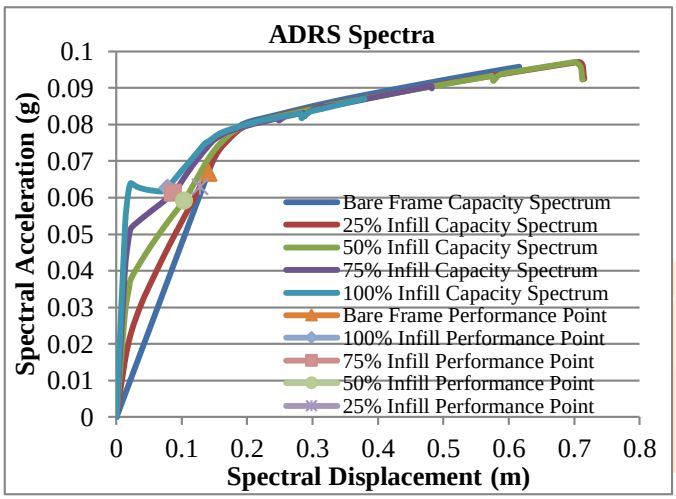

Figure 46: Performance points illustration for group (G)*

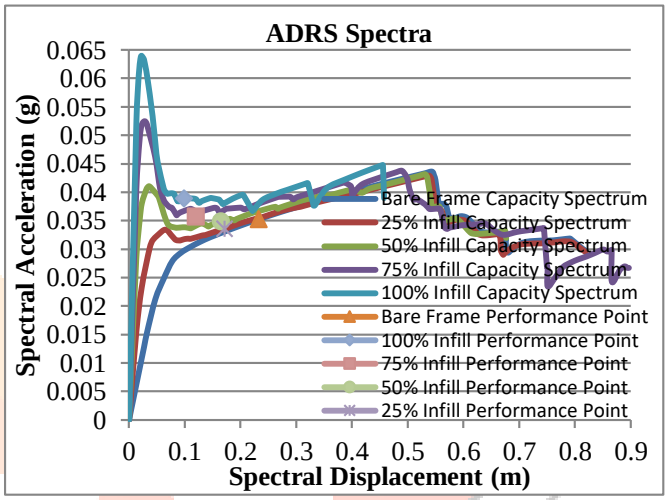

Figure 47: Performance points illustration for group (H)

Table 11: Performance points and performance levels of 10-storey height frames (* is for $k_{i.bare}$)

No. of Stories	Group	% of Infill	$k_{effect.infill}$ (ton/m)	$k_{effect.infill}/k_{i.bare}$	Performance Level	P- Factor	Increase in P-Factor (%)
10-Stories	Group (I)*	Bare Frame	424.5*		IO	5.35	0.00
		25% Infill	693.2	1.63	IO	8.18	53.06
		50% Infill	934	2.20	IO	9.99	86.88
		75% Infill	1101.2	2.59	IO	10.97	105.13
		100% Infill	1357.1	3.19	IO	12.26	129.41
	Group (J)	Bare Frame	424.5*		IO	7.07	0.00
		25% Infill	598.1	1.40	IO	9.71	37.36
		50% Infill	732.46	1.72	IO	10.96	55.13
		75% Infill	834.32	1.96	IO	11.42	61.63
		100% Infill	1166.67	2.74	IO	13.24	87.37

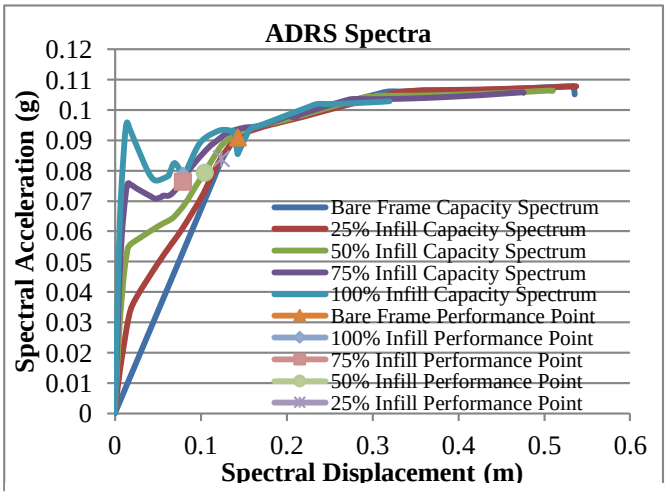

Figure 48: Performance points illustration for group (I)*

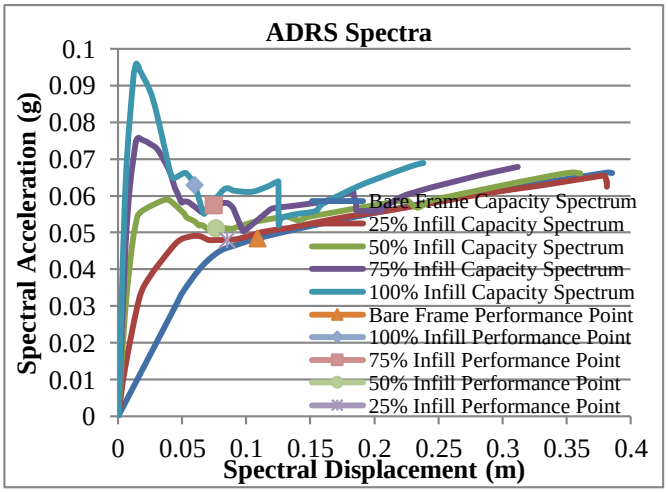

Figure 49: Performance points illustration for group (J)

4.2.5 Conclusion and Discussion

Infill contributions to the behavior of a structure under seismic events rely heavily on the initial level of performance the bare frame was originally designed upon. From analysis results it is clear that infills can contribute much effectively with CCD frames which show operational or immediate occupancy as compared to other more critically performing frames, whether life safety or collapse prevention. This could be mainly due to the fact, as mentioned in section 4.1.1.1, that CCD models show less deformation during a seismic event, obeying the drift limitations set by ECP-201and ATC-40 seismic provisions at 1%; while for life safety and collapse prevention, drift limitations are set at higher values of 2% and 0.33Vi/Pi≈ 7% respectively, as per ATC-40. In turn, infills do not crack as much with CCD frames in earlier stages of a seismic event and show more resilience to lateral deformations, hence giving a higher $k_{effect.infill}/ k_{i.bare}$ ratio and greater contribution to the P-factor. Results can be concluded in table and graphical forms as follow.

Moreover, infills can improve the performance level of the frame as already expected giving no irregularities defined in soft stories and short column effects exist. And based on the results we can conclude that overall performance level of the structure can improve with infills, slightly though; and only in cases of collapse prevention performance, frames can show a transitional level of performance with different infill percentages, changing to life safety performance.

Table 12: Effects of infills on P-factor

Performance Level	Infill Percentages	Average $k_{effect.infill}/ k_{i.bare}$	Average Increase in P-factor (%)
Immediate Occupancy	Bare Frame	1.00	0.00
	25% Infill	1.56	46.81
	50% Infill	2.05	80.48
	75% Infill	2.44	102.21
	100% Infill	2.86	119.87
Life Safety	Bare Frame	1.00	0.00
	25% Infill	1.12	9.91
	50% Infill	1.19	15.19
	75% Infill	1.40	31.95
	100% Infill	1.73	53.01
Collapse Prevention	Bare Frame	1.00	0.00
	25% Infill	1.12	7.65
	50% Infill	1.18	10.70
	75% Infill	1.38	25.46
	100% Infill	1.62	44.96

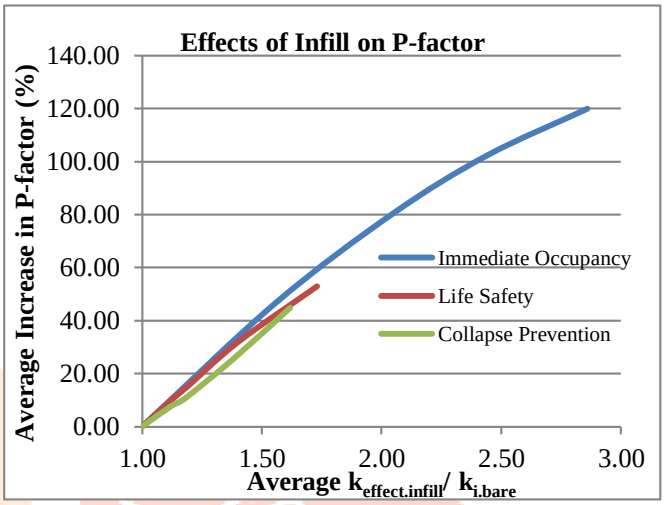

Figure 50: Effects of infills on P-factor

4.3 Effects of Infills on Overall Ductility of the Structure

URM infills crack as they deform under lateral loadings adding to the energy dissipation capacity of the frame. By definition, an increase in energy dissipation is an increase in R factor; as described before, R factor is a value assigned to different structural systems enlightens the capability of such systems in dissipating energy during a seismic event. Studies conducted in this paper show that the presence of infills can indeed increase the R factor, hence P factor, in terms of overall ductility of the structure.

Table 13: Components of P-factor for all groups

No. of Stories	Group	% of Infill	Performance Level	δ_u (m)	δ_y (m)	V_u (ton)	V_d (ton)	$R_\mu = \mu$	Ω	R_R	P- Factor
25-Stories	Group A)*	Bare Frame	IO	1.900	0.568	252.02	151.65	3.35	1.66	1	5.56
		25% Infill	IO	1.870	0.420	246.30	151.65	4.45	1.62	1	7.23
		50% Infill	IO	1.850	0.317	246.00	151.65	5.84	1.62	1	9.47
		75% Infill	IO	1.815	0.262	245.30	151.65	6.93	1.62	1	11.21
		100% Infill	IO	1.800	0.240	244.00	151.65	7.50	1.61	1	12.07
	Group B)	Bare Frame	LS (64 LS Hinges)	0.966	0.180	78.10	30.73	5.37	2.54	1	13.64
		25% Infill	LS (40 LS Hinges)	0.956	0.159	77.10	30.73	6.01	2.51	1	15.09
		50% Infill	LS (36 LS Hinges)	0.937	0.149	77.30	30.73	6.29	2.52	1	15.82
		75% Infill	LS (32 LS Hinges)	0.910	0.126	77.50	30.73	7.22	2.52	1	18.21
		100% Infill	LS (9 LS Hinges)	0.898	0.105	77.80	30.73	8.55	2.53	1	21.65
	Group C)	Bare Frame	CP (9 CP Hinges)	0.900	0.150	67.20	27.20	6.00	2.47	1	14.82
		25% Infill	LS (75 LS Hinges)	0.896	0.138	66.60	27.20	6.49	2.45	1	15.90
		50% Infill	LS (73 LS Hinges)	0.870	0.130	66.70	27.20	6.69	2.45	1	16.41
		75% Infill	LS (65 LS Hinges)	0.840	0.112	67.40	27.20	7.50	2.48	1	18.58
		100% Infill	LS (46 LS Hinges)	0.830	0.095	67.50	27.20	8.74	2.48	1	21.68
20-Stories	Group D)*	Bare Frame	IO	1.217	0.375	163.68	118.02	3.25	1.39	1	4.50
		25% Infill	IO	1.200	0.228	158.30	118.02	5.26	1.34	1	7.06
		50% Infill	IO	1.170	0.193	159.00	118.02	6.06	1.35	1	8.17
		75% Infill	IO	1.161	0.176	159.70	118.02	6.60	1.35	1	8.93
		100% Infill	IO	1.140	0.153	155.00	118.02	7.45	1.31	1	9.79

	Group E)	Bare Frame	LS (38 LS Hinges)	0.863	0.160	71.06	27.95	5.39	2.54	1	13.71
		25% Infill	LS (13 LS Hinges)	0.860	0.143	69.80	27.95	6.01	2.50	1	15.02
		50% Infill	LS (7 LS Hinges)	0.840	0.135	70.10	27.95	6.22	2.51	1	15.61
		75% Infill	IO	0.815	0.115	71.50	27.95	7.09	2.56	1	18.13
		100% Infill	IO	0.750	0.091	71.70	27.95	8.24	2.57	1	21.14
	Group F)	Bare Frame	CP (5 CP Hinges)	0.820	0.130	54.86	24.00	6.31	2.29	1	14.42
		25% Infill	LS (71 LS Hinges)	0.817	0.118	54.00	24.00	6.92	2.25	1	15.58
		50% Infill	LS (65 LS Hinges)	0.800	0.113	54.10	24.00	7.08	2.25	1	15.96
		75% Infill	LS (57 LS Hinges)	0.780	0.100	55.70	24.00	7.80	2.32	1	18.10
		100% Infill	LS (41 LS Hinges)	0.760	0.085	55.60	24.00	8.94	2.32	1	20.71
15-Stories	Group G)*	Bare Frame	IO	0.789	0.256	119.93	86.40	3.08	1.39	1	4.28
		25% Infill	IO	0.758	0.162	116.33	86.40	4.68	1.35	1	6.30
		50% Infill	IO	0.670	0.116	117.30	86.40	5.78	1.36	1	7.84
		75% Infill	IO	0.582	0.091	117.80	86.40	6.40	1.36	1	8.72
		100% Infill	IO	0.500	0.074	117.94	86.40	6.76	1.37	1	9.22
	Group H)	Bare Frame	LS (11 LS Hinges)	0.670	0.128	54.90	21.00	5.23	2.61	1	13.68
		25% Infill	IO	0.655	0.115	55.30	21.00	5.70	2.63	1	15.00
		50% Infill	IO	0.650	0.110	56.30	21.00	5.91	2.68	1	15.84
		75% Infill	IO	0.640	0.100	58.42	21.00	6.40	2.78	1	17.80
		100% Infill	IO	0.585	0.085	61.00	21.00	6.88	2.90	1	19.99
10-Stories	Group I)*	Bare Frame	IO	0.672	0.216	93.17	54.22	3.11	1.72	1	5.35
		25% Infill	IO	0.640	0.133	92.20	54.22	4.81	1.70	1	8.18
		50% Infill	IO	0.580	0.100	93.40	54.22	5.80	1.72	1	9.99
		75% Infill	IO	0.540	0.086	94.70	54.22	6.28	1.75	1	10.97
		100% Infill	IO	0.490	0.070	95.00	54.22	7.00	1.75	1	12.26
	Group J)	Bare Frame	IO	0.472	0.130	54.88	28.20	3.63	1.95	1	7.07
		25% Infill	IO	0.457	0.091	54.50	28.20	5.02	1.93	1	9.71
		50% Infill	IO	0.422	0.077	56.40	28.20	5.48	2.00	1	10.96
		75% Infill	IO	0.386	0.067	55.90	28.20	5.76	1.98	1	11.42
		100% Infill	IO	0.320	0.048	56.00	28.20	6.67	1.99	1	13.24

4.3.1 Conclusion and Discussion

Infill contribution to overall ductility can be summarized and expressed in terms of $k_{effect.infill}/ k_{i.bare}$ ratio to percentage increase in global ductility. As can be sown in the results below, effects on global ductility is very similar to the effects on P-factor; and thus it can be concluded that infills effect on P-factor is mainly due to their contribution to the global ductility of the structure.

Table 14: Effects of infills on R_μ-factor

Performance Level	Infill Percentages	Average $k_{effect.infill}/ k_{i.bare}$	Average Increase in R_μ-factor (%)
Immediate Occupancy	Bare Frame	1.00	0.00
	25% Infill	1.56	50.44
	50% Infill	2.05	83.77
	75% Infill	2.44	104.92
	100% Infill	2.86	124.51
Life Safety	Bare Frame	1.00	0.00
	25% Infill	1.12	10.78
	50% Infill	1.19	15.14
	75% Infill	1.40	29.41
	100% Infill	1.73	47.88
Collapse Prevention	Bare Frame	1.00	0.00
	25% Infill	1.12	8.99
	50% Infill	1.18	11.89
	75% Infill	1.38	24.33
	100% Infill	1.62	43.68

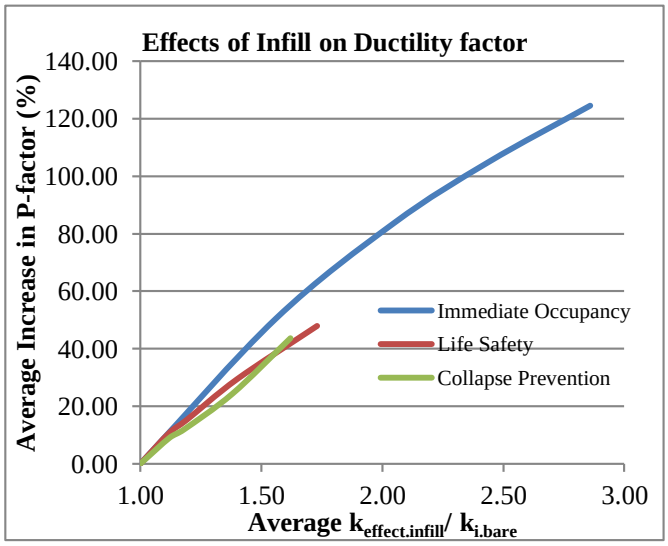

Figure 51: Effects of infills on R_μ-factor

V. SUMMARY AND CONCLUSION

Models of 2D frames of different heights were constructed to simulate the seismic demand at coastal regions of the Sinai Peninsula on the Mediterranean Sea, and to study the effects of infills during a seismic event. Effects of infills was looked in detail from four main perspectives, distinguished as: contribution of infill to energy absorption, effect on performance level, performance factor (P-factor), and global ductility (μ) during a seismic event. Groups (A, D, G and I)*, of heights 25, 20, 15 and 10 storyes respectively, are designed conforming the ECP-201 FBD design method, and are assigned the (*) notation to be distinguished as code-complaint designed (CCD) models. Groups (B and E), of heights 25 and 20 storeys respectively, are designed based on the ECP-201 lateral and vertical load combinations while neglecting minimum limitation of Horizontal Design Spectrum at $0.2*a_g*\gamma_1$. The remaining groups (C, F, H and J), of heights 25, 20, 15 and 10 storyes respectively, are designed under vertical loads only.

- Bare frames of CCD models show R-factors similar in value as suggested by ECP-201 for limited ductility at R=5.
- CCD frames show less deformation as they abide by the more conservative drift limits set by ECP-201 and ATC-40, and hence infills experience less damage during a seismic event at earlier stages of pushover analysis.
- CCD frames show immediate occupancy (IO) performance levels based on the guidelines set by FEMA-356 and ATC-40.
- As a result, CCD frames can absorb much higher percentage of seismic energy than the infills as compared to other less performing frames, thus leaving infills less susceptible to early damage during an earthquake.
- Infill contributions to the behavior of a structure under seismic events rely heavily on the initial level of performance the bare frame was originally designed upon (immediate occupancy level, life safety level, and collapse prevention level).
- Infills, therefore, show higher contribution to the behavior of the CCD frames in terms of global ductility (μ) and performance factor (P).
- Infills have minimal, if no, effect on over strength component (**Ω**) of the (R or P) factor.
- Energy dissipation owing to infill cracks and damage is mainly computed in terms of contribution to global ductility (μ).
- Infills can improve performance level of frames given that no irregularities in terms of neither soft-story nor short column effects exist.

VI. REFERENCES

[1] CEB (1996), RC Frames Under Earthquake Loading - State of the Art Report, Comite Euro-International Du Beton, Thomas Telford, UK.

[2] CEN (1994), Eurocode 8 - Design Provisions for Earthquake Resistance of Structures, European Committee for Standardisation, Brussels.

[3] Murty, C.V.R., and Nagar, A. (1996), "Effect of Brittle Masonry Infills on Displacement and Ductility Demand of Moment Resisting Frames," Proceedings of Eleventh World Conference on Earthquake Engineering, Acapulco, Mexico.

[4] Dr. Saraswati Setia and Vineet Sharma, (2012), "Seismic Response of R.C.C Building with Soft Storey", International Journal of Applied Engineering Research, ISSN 0973-4562 Vol.7 No.11, Kanpur, India.

[5] Murty, C.V.R., (1996), "Why are Short Columns more damaged during Earthquakes?" Indian Institute of Technology, Kanpur, India.

[6] Marina L. Moretti, Georgios Mousafiropoulos, Theodoros Fotakopoulos, and Triantafyllos K. Makarios, (2013), "Influence of masonry infills in torsional irregular RC buildings Part 2: Analysis and results according to the Eurocodes", The 2013 World Congress on Advances in Structural Engineering and Mechanics (ASEM13), Jeju, Korea.

[7] R.B.Ghodke, Prof. M.V.Waghmare, Prof. U.R.Awari, (2016), "Torsional Effect for Unsymmetrical R.C. Frames", International Research Journal of Engineering and Technology (IRJET), India.

[8] FEMA - 306: "Evaluation of Earthquake Damaged Concrete and Masonry Wall Buildings - Basic Procedures Manual" Federal Emergency Management Agency, 1999.

[9] C.V .R Murty and Sudhir K JAIN2, (2000), "Beneficial Influence of Masonry Infill Walls on Seismic Performance of RC Frame Buildings", 12th World Conference on Earthquake Engineering (12WCEE 2000), Kanpur, India.

[10] M.J.N and Priestley, (2000), "Performance Based Seismic Design", 12th World Conference on Earthquake Engineering (12WCEE 2000), University of California, San Diego.

[11] Park R. and Paulay T (1975), "Reinforced Concrete Structures", John Wiley & Sons. New York, 769 p.

[12] Paulay, T. (1997) "A behaviour-based design approach to earthquake-induced torsion in ductile buildings" In Fajfar P. and Krawinkler, H (Eds) (1997), "Seismic Design Methodologies for the Next Generation of Codes". Proceedings of International Conference at Bled, Slovenia. A.A. Balkema, Rotterdam/Brookfield, 1997, pp289-298.

[13] Mehmed Causevic and Sasa Mitrovic, (2010), "Comparison between non-linear dynamic and static seismic analysis of structures according to European and US provisions", Springer Science+ Business Media B.V. 2010, Rijeka, Croatia.

[14] Fajfar P (2000) "A nonlinear analysis method for performance based seismic design", Earthq Spectra 16(3):573– 592.

[15] Abdelatee Eljadei, (2012), "Performance Based Design of Coupled Wall Structures", Research Gate, Pennsylvania, United States.

[16] ATC 40: "Seismic Evaluation and Retrofit of Concrete Buildings" Applied Technology Council, California, USA, 1996.

[17] Roberto Gentile, Stefano Pampanin, Domenico Raffaele, Giuseppina Uva (2019), "Non-linear analysis of RC masonry-infilled frames using the SLaMA method: part 1—mechanical interpretation of the infill/frame interaction and formulation of the procedure," Bulletin of Earthquake Engineering (2019) 17:3283–3304, Springer.

[18] H.R. Lotfi and P.B. Shing (1991), "An appraisal of smeared crack models for masonry shear wall analysis", Department of Civil, Environmental, and Architectural Engineering, University of Colorado,USA

[19] Armin B. Mehrabi and P.B. Shing (1997), "Finite Element Modeling of Masonry-Infilled RC Frames", Journal of Structural Engineering, University of California, USA

[20] Paulo B. Lourence and J.G. Rots (1995), "Two approaches for the analysis of masonry structures: Micro and macro-modeling", Delft University of Technology, Faculty of Civil Engineering, the Netherlands

[21] Paulo B. Lourence and J.G. Rots (1995), "FINITE ELEMENT ANALYSIS OF MASONRY STRUCTURES: PART I- REVIEW OF PREVIOUS WORK", Ninth North American Masonry Conference, Clemson, South Carolina, USA
[22] Francisco Crisafulli (1997), "Seismic behaviour of reinforced concrete structures with masonry infills", University of Canterbury Library, National University of Canterbury, New Zealand
[23] Polyakov, S.V. (1960). "On the Interactions between masonry filler walls and enclosing frame when loaded in the plane on the wall", Translations in Earthquake Engineering, Earthquake Engineering Research Institute, San Francisco, USA, pp. 36-42.
[24] M. Holmes (1961), "Steel Frames with brickwork and concrete infilling", Proceedings of the Institution of Civil Engineers
[25] Richard Evans. Klingner (1977), "Infilled frames in earthquake-resistant construction", University of California, Berkeley, USA
[26] Liauw Te-Chang and Kwan Kwok-Hung (1984), "Nonlinear behaviour of non-integral infilled frames", Computers and Structures, vol. 18, pp. 551-560, 1984
[27] Zarnic R, Tomazevic M (1984), "The behavior of masonry infilled reinforced concrete frames subjected to cyclic lateral loading", Proc Ninth World Conf. on Earthq. Eng, San Francisco, USA, VI, 863-870
[28] Abolghasem Saneinejad and B. Hobbs (1995), "Inelastic Design of Infilled Frames", Journal of Structural Engineering-ASCE, USA
[29] FEMA - 356: "Pre standard and Commentary for the Seismic Rehabilitation of Buildings", Federal Emergency Management Agency, 2000
[30] ASCE 41-17: "Seismic Evaluation and Retrofit of Existing Buildings", American Society of Civil Engineers, Reston, VA, USA, 2017
[31] ECP-201: "Egyptian Code for Calculation of Loads and Forces for Buildings", Egypt, 2008
[32] T. B. Panagiotakos and M. N. Fardis (2001), "Deformation of Reinforced Concrete Members at Yielding and Ultimate", ACI Structural Journal, University of Patras, Greece